Connecting orbit structure of monotone solutions in the shadow system*

Hiroshi Kokubu[†]
Department of Mathematics,
Kyoto University, Kyoto 606-01, Japan

Konstantin Mischaikow[‡]
Center for Dynamical Systems and Nonlinear Studies
School of Mathematics, Georgia Institute of Technology
Atlanta, GA 30332, U.S.A.

Yasumasa Nishiura
Laboratory of Nonlinear Studies and Computation
Research Institute for Electronic Science
Hokkaido University, Sapporo 060, Japan

Hiroe Oka[§]
Department of Applied Mathematics and Informatics
Faculty of Science and Technology
Ryukoku University, Seta, Otsu 520-21, Japan

and

Takeshi Takaishi
Faculty of Engineering
Hiroshima-DENKI Institute of Technology
Aki-ku, Hiroshima 739-03, Japan

July 4, 1996

Abstract

The shadow system

$$\begin{aligned} u_t &= \varepsilon^2 u_{xx} + f(u) - \xi, \\ \xi_t &= \int_I g(u,\xi)dx, \end{aligned} \qquad I = [0,1]$$

is a scalar reaction diffusion equation coupled with an ODE. The extra freedom coming from the ODE drastically influences the solution structure and dynamics as compared to that of a single scalar reaction diffusion system. In fact, it causes secondary bifurcations and coexistence of multiple stable equilibria. Our long term goal is a complete description of the global dynamics on its global attractor $\mathcal{A}$ as a function of ϵ, f, and g. Since this is still far beyond our capabilities, we focus on describing the dynamics of solutions to the shadow system which are monotone in x, and classify the global connecting orbit structures in the monotone solution space up to the semi-conjugacy. The maximum principle and hence the lap number arguments, which have played a central role in the analysis of one dimensional scalar reaction diffusion equations, cannot be directly applied to the shadow system, although there is a Lyapunov function in an appropriate parameter regime. In order to overcome this difficulty, we resort to the Conley index theory. This method is topological in nature, and allows us to reduce the connection problem to a series of algebraic computations. The semi-conjugacy property can be obtained once the connection problem is solved. The shadow system turns out to exhibit minimal dynamics which displays the mechanism of basic pattern formation, namely it explains the dynamic relation among the trivial rest states (constant solutions) and the event patterns (large amplitude inhomogeneous solutions).

*Research was supported in part by NSF Grant INT-9315117 and JSPS US-Japan Cooperative Research MPCR-294.

†Research was supported in part by Grant-in-Aid for Scientific Research (No. 06740150, 07740150, 08740139), Ministry of Education, Science and Culture, Japan.

‡Research was supported in part by NSF Grants DMS-9101412, DMS-9302970, and DMS-9505116.

§Research was supported in part by Science and Technology Fund for Research Grants of Ryukoku University, and by Grant-in-Aid for Scientific Research (No. 07640338, 08640143), Ministry of Education, Science and Culture, Japan.

1 Introduction

One of the ultimate goals in the Pattern Formation Problem is to understand the global dynamics of the phenomena of interest. For instance, let us consider a "threshold phenomena", namely, there is a critical trigger level which causes an event. If the critical level is exceeded, some pattern of finite size, e.g. a stationary or travelling wave, is formed from the trigger, but on the other hand, everything dies out and tends to the rest state when the threshold level is not reached.

In order to clarify this phenomenon, first we should know the *existence* and *local stability properties* of rest, event, and threshold patterns respectively. In particular, it is important to know the dimension of the unstable manifold of the threshold pattern, since its stable manifold plays a separatrix-like role in the system. Second, we must solve the *connection problem* among those solutions, in particular, we have to show that the unstable manifold of the threshold pattern is connected to the event and rest patterns, respectively. The third step is to show that the dynamics exhibited by the system is *conjugate* (or *semi-conjugate*) to a lower dimensional model flow. Not only for the threshold phenomenon but also in more general contexts, the above three steps are crucial in the study of the global dynamic behavior exhibited by the system. The aim of this paper is to understand the global dynamics of the following system (called the *shadow system*) according to the above scenario. Our primary focus is on the connection and conjugacy problems. We consider the equation

$$\begin{array}{rcl} u_t & = & \varepsilon^2 u_{xx} + f(u) - \xi, \\ \xi_t & = & \displaystyle\int_I g(u,\xi)dx, \end{array} \qquad (t,x) \in [0,+\infty) \times I, \ I = [0,1] \tag{1}$$

subject to the Neumann boundary condition on ∂I, where ξ is a spatially constant function in t. Here the nonlinearity takes the following special but still fairly typical form:

$$f(u) = ku - u^3, \tag{2}$$

$$g(u,\xi) = \lambda u + \mu - \xi, \tag{3}$$

where $\lambda (> 0)$ and μ are the bifurcation parameters, and $\varepsilon > 0$ and $0 < k < 1$ are constants. Here ε is not necessarily small, but should belong to an appropriate region. See Proposition 1.1. Originally the system (1) was introduced in [18] as a limiting system of the full reaction diffusion system when the diffusivity of the inhibitor tends to infinity. Although (1) is much simpler than the full system, it still keeps several essential features of the original system, for instance, it has stable spatially inhomogeneous solutions making a sharp contrast with the scalar case. Moreover, (1) becomes one of the organizing centers that produce the skeleton structure of solutions to the full system (see [19] for details). Despite its simple appearance, (1) displays a variety of steady states and dynamics depending on the parameters λ and μ. For all parameter values this system possesses a global attractor which we shall denote by $\mathcal{A}$. Our long term goal is a complete description of the global dynamics on $\mathcal{A}$ as a function of the parameter values λ and μ. Since this is still far beyond our capabilities we restrict our attention in this paper to describing the dynamics of solutions to the shadow system which are monotone in x. As will be shown in the next section the space of monotone solutions, which we denote by $\mathcal{M}$ is positively invariant in $\mathcal{A}$. Thus, the set of solutions we will study is the maximal invariant set in $\mathcal{M}$ which we shall denote by $\mathcal{A}_{\mathcal{M}}$.

Even restricted to the monotone solution subspace, the extra freedom coming from the ODE of the shadow system drastically influences the structure of the equilibrium solutions and the dynamics as compared to that of a single scalar reaction diffusion equation. In fact, it causes secondary bifurcations and the coexistence of multiple stable equilibria (see [18], [20]). In particular, (1) contains a threshold phenomenon in an appropriate parameter regime. On the other hand, we have to pay a cost for this rich structure, namely, the maximum principle and hence the lap number arguments cannot be directly applied to (1), although there is a Lyapunov function in an appropriate parameter regime. Therefore, the arguments employed in [2] cannot be applied directly to our problem. In order to overcome this difficulty, we resort to the Conley index theory [3] and in particular make extensive use of the "connection matrix" as developed in [4]–[7]. The nature of this method is topological, and hence it allows the connection problem to be reduced to algebraic computations. The semi-conjugacy can be determined once the connection problem is solved. The dynamics of (1) turns out to be a minimal one which displays the mechanism of the basic pattern formation, namely it explains the dynamic relation among the trivial rest states (constant solutions) and the event patterns (large amplitude inhomogeneous solutions).

The first result of the next section is that for $0 < \lambda < 1$ the shadow system possesses a Lyapunov function, and hence, is gradient–like. This implies that $\mathcal{A}$ consists of equilibria and connecting orbits between these equilibria. Thus the first question which needs to be addressed is what are the equilibria for the various parameter values. Due to the work of [18]–[21], there are three different kinds of solutions denoted by A, B, and C, respectively. Loosely speaking, for sufficiently small ε, A corresponds to interior transition layered solutions, B to boundary layered solutions, and C to constant solutions. These three classes of solutions are furthermore divided into several types as follows: the superscript

$^+$ refers to a monotone increasing solution, whereas $^-$ a monotone decreasing solution; C^a stands for a constant solution with a larger value (than the other constant solutions), C^b the one with a smaller value, and C the one with a middle value; finally, B^{+a} stands for a monotone increasing solution which is close to C^a, etc. See Figure 1 for the wave profiles of some stationary solutions. There is an ambiguity in this classification of solutions, namely two solutions belonging to different classes merge at bifurcation points (of saddle-node or pitchfork type) as we will see in the next proposition. However, there is no confusion if we assume that those names are given to each connected component, except merging points, of solution branch containing, say, boundary layered solutions.

The next proposition shows how these solutions emerge from constant states, or merge via saddle-node bifurcations. See Figure 2 for the bifurcation sets. The proof of the proposition is omitted, since it is straightforward with the aid of [18]–[21] and the monotone property of [25]. The parameter ε should not be very large, otherwise interesting patterns do not occur. In what follows we assume that ε is appropriately small, but not necessarily very small, so that the next proposition holds.

Proposition 1.1 *1. At the curve $S_{C\pm} : \frac{(\lambda-k)^3}{27} + \frac{\mu^2}{4} = 0$, a saddle-node bifurcation occurs and stationary solutions C and C^a (if $\mu > 0$) or C and C^b (if $\mu < 0$) appear. This saddle-node bifurcation reduces to the pitchfork bifurcation when $\mu = 0$, which produces C^a and C^b from C.*

2. *At the line $P_{C+} : \mu = \sqrt{\frac{k}{3}}(\lambda - \frac{2k}{3})$, the stationary solution C^b undergoes a pitchfork bifurcation and produces $B^{\pm b}$. Similarly at $P_{C-} : \mu = -\sqrt{\frac{k}{3}}(\lambda - \frac{2k}{3})$, the stationary solution C^a undergoes a pitchfork bifurcation and producing $B^{\pm a}$.*

3. *Finally, at a curve $S_{AB+} : \mu \approx \sqrt{k}\lambda$, there occurs another saddle-node bifurcation involving $A^\pm$ and $B^{\pm b}$ respectively. In the same way, a saddle-node bifurcation producing $A^\pm$ and $B^{\pm a}$, respectively, occurs at a curve $S_{AB-} : \mu \approx -\sqrt{k}\lambda$.*

Based on the information for the bifurcations of stationary solutions given in the previous proposition, we have the following list of stationary solutions appearing in each of the parameter regions decomposed by the bifurcation curves.

Proposition 1.2 *In each of the parameter regions shown in Figure 2, we have*

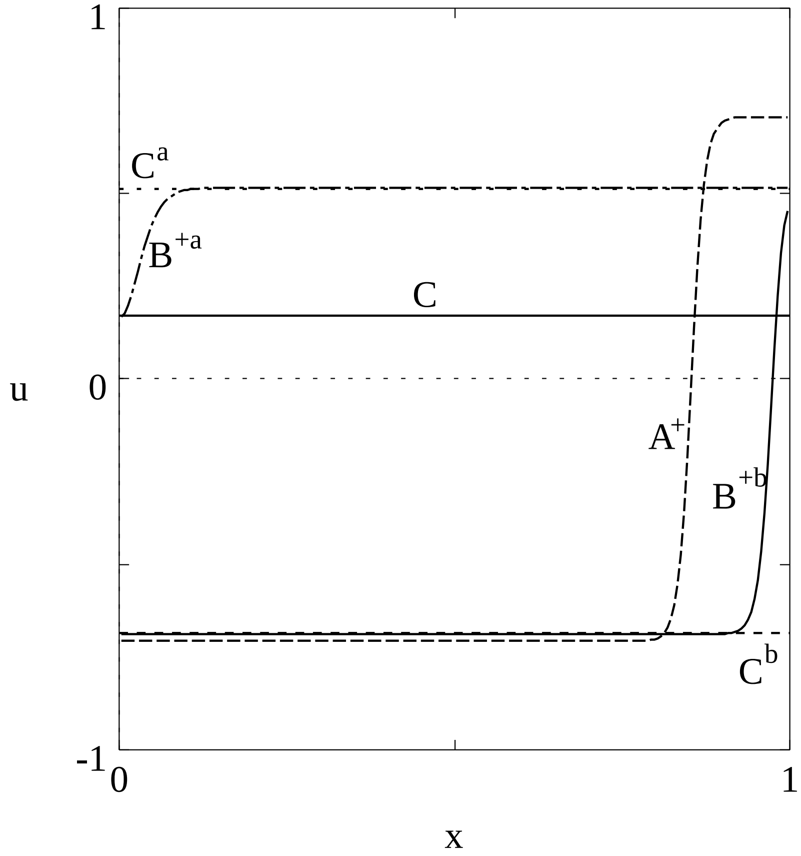

Figure 1: Wave profiles of stationary solutions for the parameter values $k = 0.5,\ \varepsilon = 0.01,\ \lambda = 0.12,\ \mu = 0.06$.

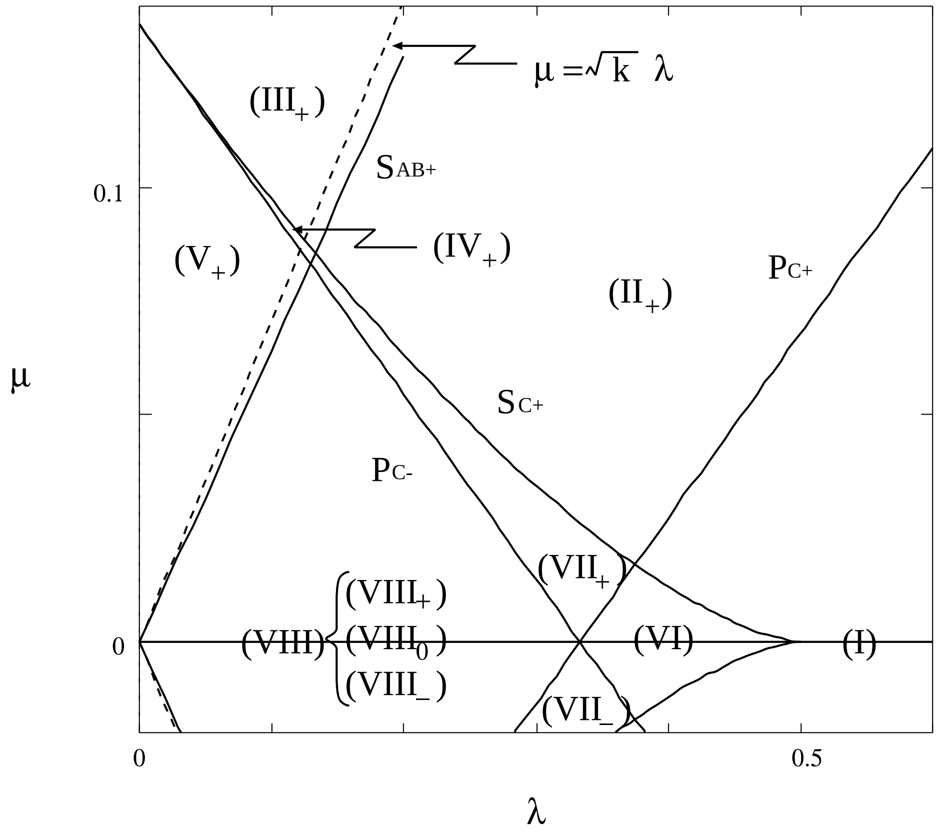

Figure 2: Bifurcation sets for the shadow system with k=0.5.

the following steady solutions:

$$\begin{array}{ccl}
\mathrm{I} & : & C, A^+, A^- \\
\mathrm{II}_+ & : & C^b, A^+, A^-, B^{+b}, B^{-b} \\
\mathrm{II}_- & : & C^a, A^+, A^-, B^{+a}, B^{-a} \\
\mathrm{III}_+ & : & C^b \\
\mathrm{III}_- & : & C^a \\
\mathrm{IV}_+ & : & C, C^a, C^b \\
\mathrm{IV}_- & : & C, C^a, C^b \\
\mathrm{V}_+ & : & C, C^a, C^b, B^{+a}, B^{-a} \\
\mathrm{V}_- & : & C, C^a, C^b, B^{+b}, B^{-b} \\
\mathrm{VI} & : & C, A^+, A^-, C^a, C^b \\
\mathrm{VII}_+ & : & C, A^+, A^-, C^a, C^b, B^{+b}, B^{-b} \\
\mathrm{VII}_- & : & C, A^+, A^-, C^a, C^b, B^{+a}, B^{-a} \\
\mathrm{VIII} & : & C, A^+, A^-, C^a, C^b, B^{+a}, B^{+b}, B^{-a}, B^{-b}
\end{array}$$

Table 1 which, again, is due to [19, 20, 21] indicates the number of unstable eigenfunctions which lie in the subspace of monotone functions for each of these solutions in the respective region. Figures 3 and 4 exhibit the qualitative aspect of the null-clines of the nonlinearity f and g.

The goal of this paper is to prove the following theorems which provide a qualitative description of the global dynamics of the monotone solutions to the shadow system. These theorems are obtained by combining analytical and topological methods from dynamical systems, with the help of numerical computations at some points. The advantage of employing topological methods lies in the fact that certain homological information of the attractors greatly restricts the possible types of connecting orbits among equilibrium points in the attractors. It appears that to use only analytic methods would require more complicated arguments. In fact, one of our theorems gives a simplified proof of some earlier results (Gardner et al. [8]) on the connecting orbit structure.

Since the structure of $\mathcal{A}_{\mathcal{M}}$ varies as a function of the parameters we will let $\mathcal{A}_{\mathcal{M}}(i)$ denote $\mathcal{A}_{\mathcal{M}}$ for the parameter values in the regions $i =$ I, II$_\pm$, III$_\pm$, IV$_\pm$, V$_\pm$, VI, VII$_\pm$, VIII.

In the following theorems we characterize the dynamics on $\mathcal{A}_{\mathcal{M}}$ in terms of conjugacies and semi-conjugacies. Recall that a flow $\varphi : \mathbf{R} \times X \to X$ is *semi-conjugate* to $\psi : \mathbf{R} \times Y \to Y$ if there exists a continuous surjective mapping $\rho : X \to Y$ such that the following diagram commutes,

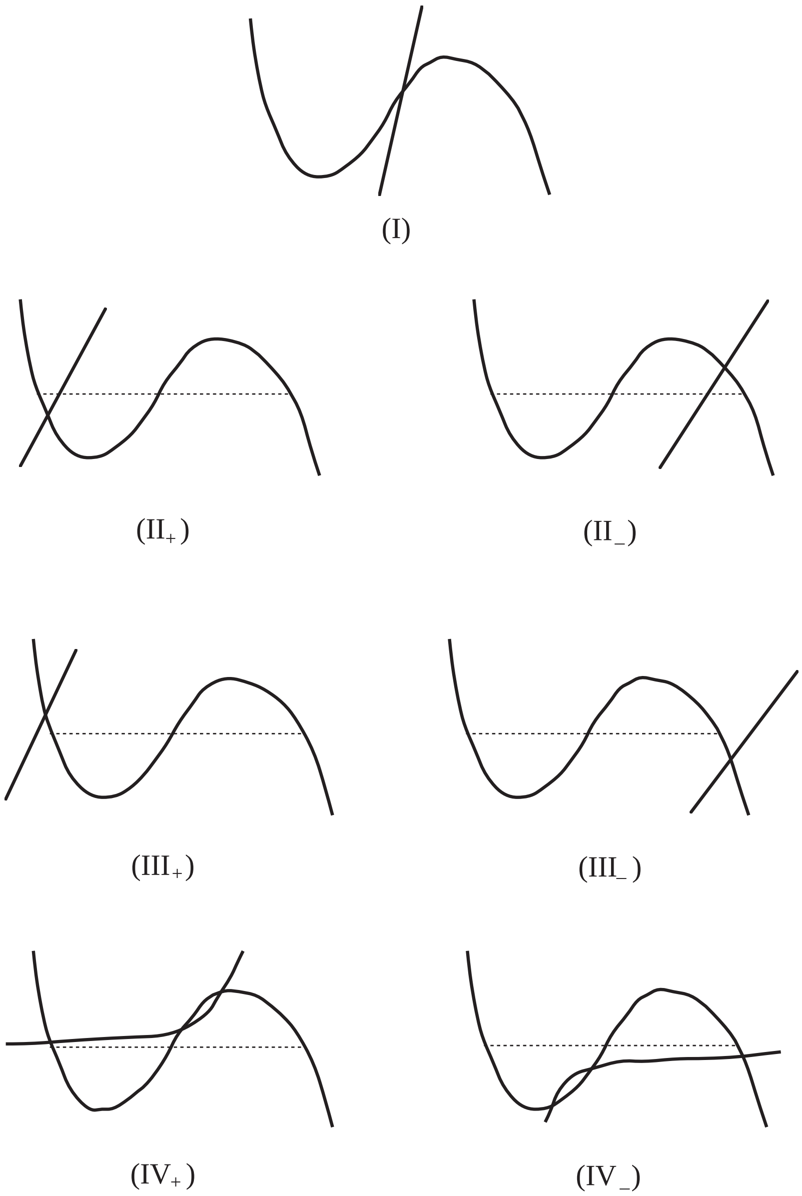

Figure 3: Qualitative aspects of the curves $f(u, \xi) = 0$ and $g(u, \xi) = 0$ in each of the parameter regions.

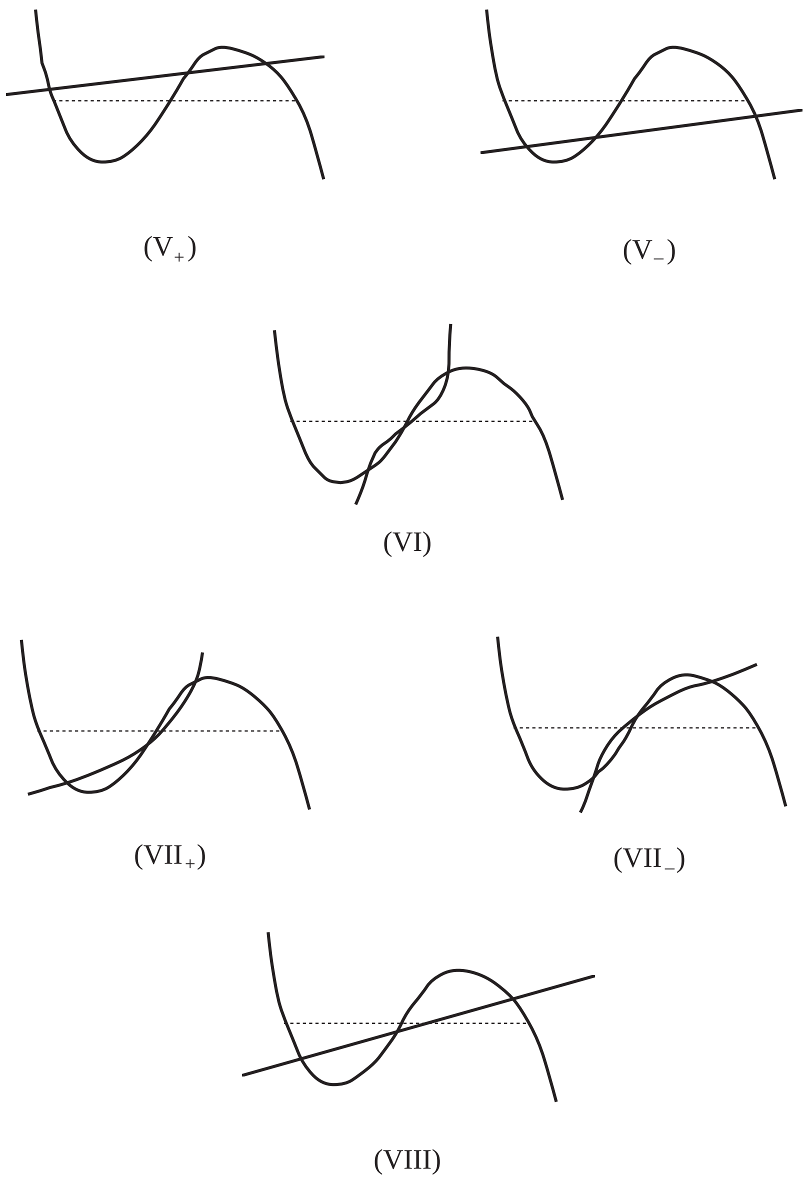

Figure 4: Qualitative aspects of the curves $f(u, \xi) = 0$ and $g(u, \xi) = 0$ in each of the parameter regions (continued).

$$\mathrm{A}^{-} \longleftarrow \mathrm{C} \longrightarrow \mathrm{A}^{+}$$

Figure 5: A flow conjugate to $\mathcal{A}_{\mathcal{M}}(\mathrm{I})$.

region	C	C^a	C^b	A^+	A^-	B^{+a}	B^{-a}	B^{+b}	B^{-b}
I	1			0	0				
II_+			0	0	0			1	1
II_-		0		0	0	1	1		
III_+			0						
III_-		0							
IV_+	2	1	0						
IV_-	2	0	1						
V_+	2	0	0			1		1	
V_-	2	0	0				1		1
VI	2	1	1	0	0				
VII_+	2	1	0	0	0			1	1
VII_-	2	0	1	0	0	1	1		
VIII	2	0	0	0	0	1	1	1	1

Table 1: The number of monotone unstable eigenfunctions in the respective regions of parameter space. Vacant boxes indicate that the steady state solutions do not occur in those regions.

$$A^- \longleftarrow B^{-b} \longrightarrow C \longleftarrow B^{+b} \longrightarrow A^+$$

Figure 6: A flow conjugate to $\mathcal{A}_{\mathcal{M}}(\mathrm{II}_+)$.

$$A^- \longleftarrow B^{-a} \longrightarrow C \longleftarrow B^{+a} \longrightarrow A^+$$

Figure 7: A flow conjugate to $\mathcal{A}_{\mathcal{M}}(\mathrm{II}_-)$.

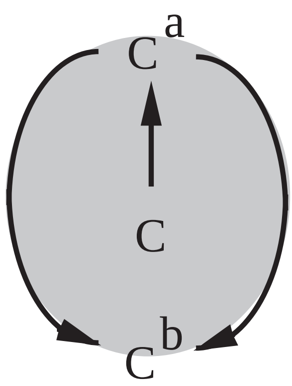

Figure 8: The flow to which $\mathcal{A}_{\mathcal{M}}(\mathrm{IV}_+)$ is semi-conjugate.

$$\begin{tikzcd}
\mathbf{R} \times X \arrow[r, "\varphi"] \arrow[d, "id \times \rho"'] & X \arrow[d, "\rho"] \\
\mathbf{R} \times Y \arrow[r, "\psi"] & Y
\end{tikzcd}$$

If ρ is a homeomorphism, then φ is *conjugate* to ψ. In our results φ will be the flow on $\mathcal{A}_{\mathcal{M}}$, while ψ will be an explicit flow defined on the unit interval or a subset of $\mathbf{R}^2$. Conjugacy between flows is a very strong relation since it implies that on the topological level the dynamics in the two systems is identical. We are only able to demonstrate the existence of a conjugacy in Theorems 1.3 and 1.4. In the other cases our description is in terms of semi-conjugacies. This is obviously a much weaker description, however it should be observed that it does provide a lower bound on the complexity of the dynamics in $\mathcal{A}_{\mathcal{M}}$. This can be seen by noting that since ρ is surjective, for any orbit in ψ, in its preimage under ρ there exists at least one and perhaps a set of corresponding orbits in φ.

Theorem 1.3 *The dynamics on $\mathcal{A}_{\mathcal{M}}(\mathrm{I})$, $\mathcal{A}_{\mathcal{M}}(\mathrm{II}_+)$ and $\mathcal{A}_{\mathcal{M}}(\mathrm{II}_-)$ are conjugate to the flows on the unit interval indicated in Figures 5, 6 and 7, respectively.*

Theorem 1.4 *The maximal invariant sets $\mathcal{A}_{\mathcal{M}}(\mathrm{III}_+)$ and $\mathcal{A}_{\mathcal{M}}(\mathrm{III}_-)$ consist of single points C^b and C^a, respectively, and are globally attracting.*

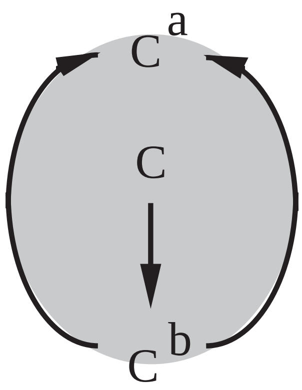

Figure 9: The flow to which $\mathcal{A}_{\mathcal{M}}(\mathrm{IV}_{-})$ is semi-conjugate.

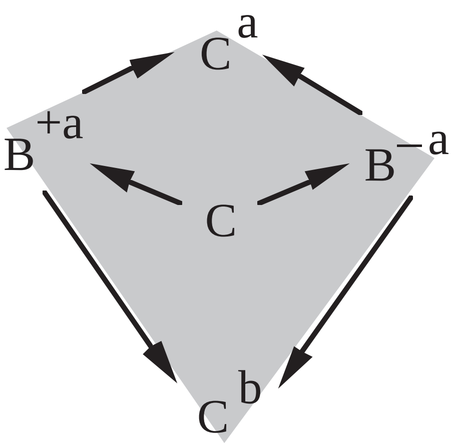

Figure 10: The flow to which $\mathcal{A}_{\mathcal{M}}(\mathrm{V}_{+})$ is semi-conjugate.

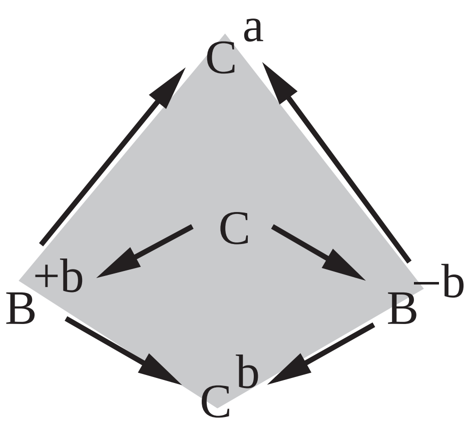

Figure 11: The flow to which $\mathcal{A}_{\mathcal{M}}(\mathrm{V}_{-})$ is semi-conjugate.

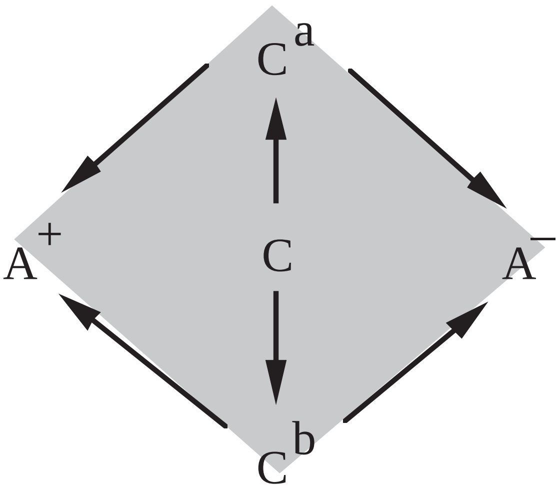

Figure 12: A flow to which $\mathcal{A}_{\mathcal{M}}(\mathrm{VI})$ is semi-conjugate.

Theorem 1.5 *The dynamics on* $\mathcal{A}_{\mathcal{M}}(\mathrm{IV}_+)$ *and* $\mathcal{A}_{\mathcal{M}}(\mathrm{IV}_-)$ *are semi-conjugate to the planar flows on the unit disk indicated in Figures 8 and 9, respectively.*

Theorem 1.6 *The dynamics on* $\mathcal{A}_{\mathcal{M}}(\mathrm{V}_+)$ *and* $\mathcal{A}_{\mathcal{M}}(\mathrm{V}_-)$ *are semi-conjugate to the planar flows indicated in Figures 10 and 11, respectively.*

Theorem 1.7 *The dynamics on* $\mathcal{A}_{\mathcal{M}}(\mathrm{VI})$ *is semi-conjugate to the planar flow indicated in Figure 12.*

Theorem 1.8 *(1) The dynamics on* $\mathcal{A}_{\mathcal{M}}(\mathrm{VII}_+)$ *is semi-conjugate to one of the planar flows indicated in Figure 13(a), (b), or (c) where in the latter case* C*,* $A^{\pm}$*, and* $B^{\pm b}$ *are mapped to the fixed point* $M(*)$*. If, furthermore,* $\mathcal{A}_{\mathcal{M}}(\mathrm{VII}_+)$ *is a two dimensional graph over the subspace spanned by the two monotone unstable eigenfunctions of* C*, then the same conclusion holds except that Figure 13(c) may be replaced by Figure 13(d).*
(2) The dynamics on $\mathcal{A}_{\mathcal{M}}(\mathrm{VII}_-)$ *is semi-conjugate to one of the planar flows indicated in Figure 14(a), (b), or (c) where in the latter case* C*,* $A^{\pm}$*, and* $B^{\pm a}$ *are mapped to the fixed point* $M(*)$*. If, furthermore,* $\mathcal{A}_{\mathcal{M}}(\mathrm{VII}_-)$ *is a two dimensional graph over the subspace spanned by the two monotone unstable eigenfunctions of* C*, then the same conclusion holds except that Figure 14(c) may be replaced by Figure 14(d).*

Warning: The following “theorem” was “proven” with the aid of a simple numerical computation which was not verified with full mathematical rigor. The results of the numerical computation should not, however, be hard to justify, perhaps by careful error estimates. This comment will be explained in detail in §4.

Theorem 1.9 *(1) The dynamics on* $\mathcal{A}_{\mathcal{M}}(\mathrm{VIII}_0)$ *is semi-conjugate to the planar flow indicated in Figure 15.*
(2) The dynamics on $\mathcal{A}_{\mathcal{M}}(\mathrm{VIII}_+)$ *is semi-conjugate to one of the planar flows indicated in Figure 16(a), (b), or (c) where in the latter case* C*,* $A^{\pm}$*, and* $B^{\pm b}$ *are mapped to the fixed point* $M(*)$*. If, furthermore,* $\mathcal{A}_{\mathcal{M}}(\mathrm{VIII}_+)$ *is a two dimensional graph over the subspace spanned by the two monotone unstable eigenfunctions of* C*, then the same conclusion holds except that Figure 16(c) may be replaced by Figure 16(d).*
(3) The dynamics on $\mathcal{A}_{\mathcal{M}}(\mathrm{VIII}_-)$ *is semi-conjugate to one of the planar flows indicated in Figure 17(a), (b), or (c) where in the latter case* C*,* $A^{\pm}$*, and* $B^{\pm a}$ *are mapped to the fixed point* $M(*)$*. If, furthermore,* $\mathcal{A}_{\mathcal{M}}(\mathrm{VIII}_-)$ *is a two dimensional graph over the subspace spanned by the two monotone unstable eigenfunctions of* C*, then the same conclusion holds except that Figure 17(c) may be replaced by Figure 17(d).*

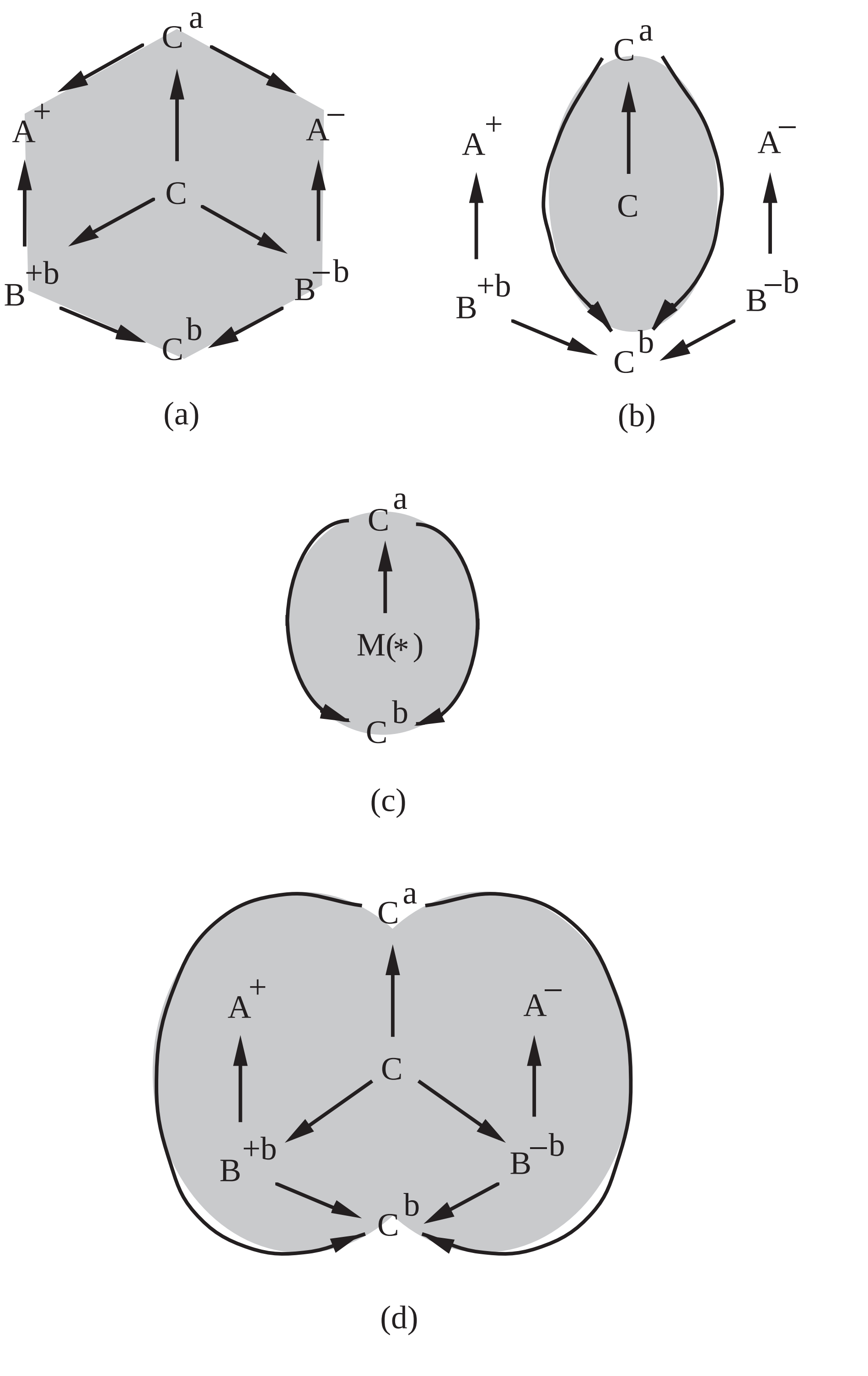

Figure 13: Three flows, to one of which $\mathcal{A}_{\mathcal{M}}(\mathrm{VII}_+)$ is semi-conjugate.

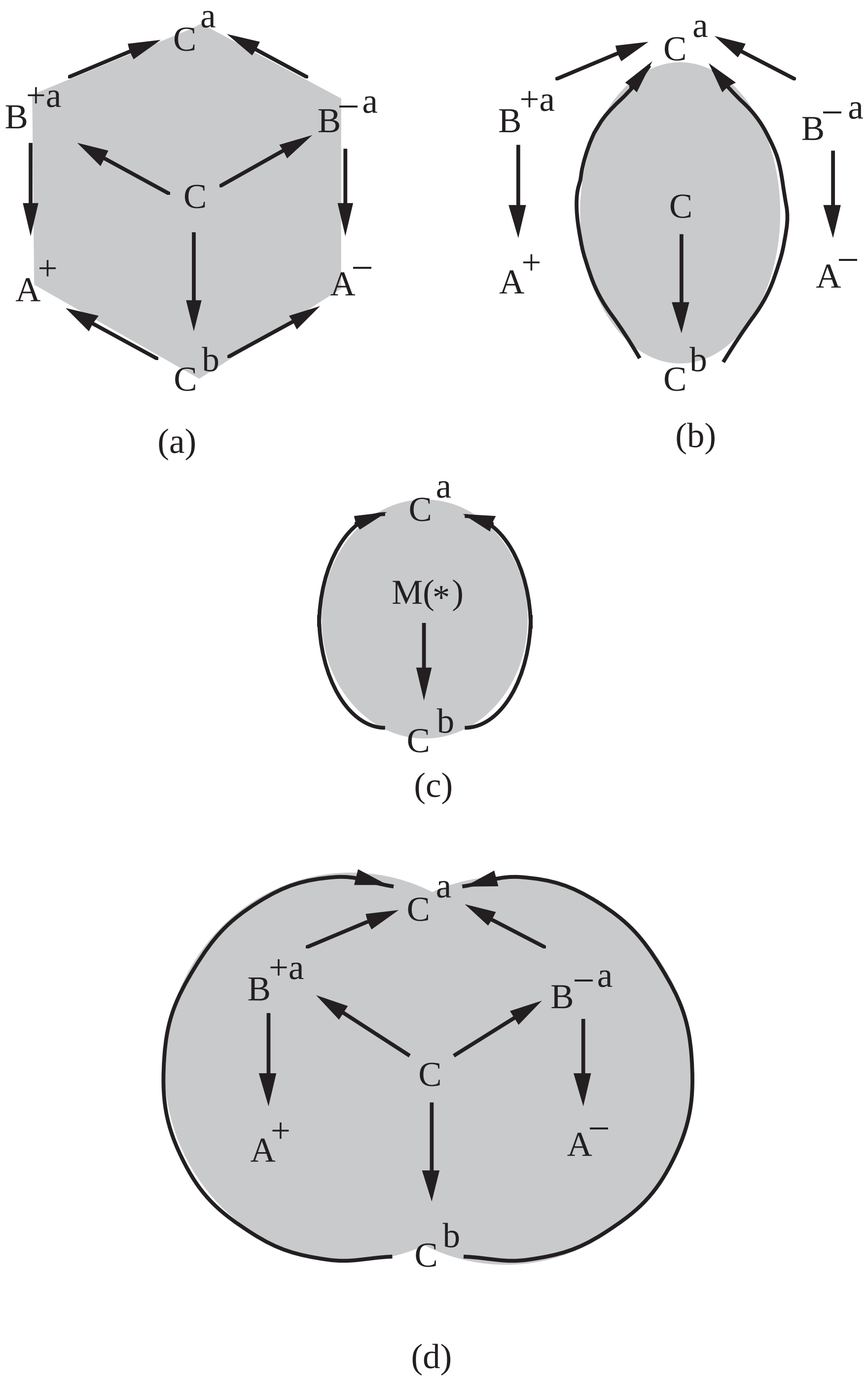

Figure 14: Three flows, to one of which $\mathcal{A}_{\mathcal{M}}(\mathrm{VII}_{-})$ is semi-conjugate.

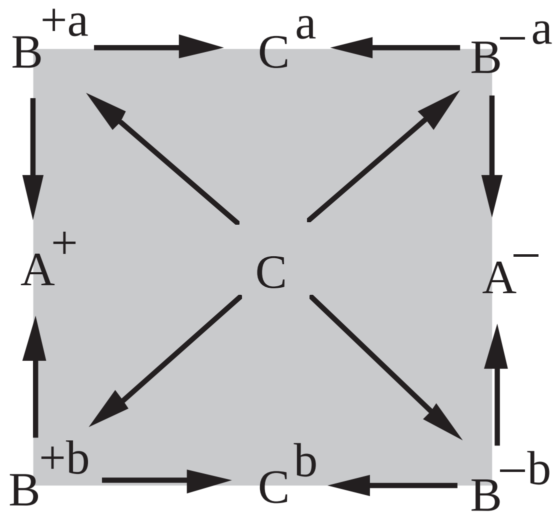

Figure 15: A flow to which $\mathcal{A}_{\mathcal{M}}(\mathrm{VIII}_0)$ is semi-conjugate.

It may be important to emphasize that these theorems are proven by combining the three different kinds of ingredients, namely analytical properties of the shadow system, some qualitative studies of topological semi-flows using the Conley indices, and the results of robust numerical computations for particular connecting orbits based on the knowledge of the orbit structure obtained from the former two methods.

The structure of the rest of this paper is as follows. First we summarize fundamental properties of the shadow system in §2, and give a brief review of the relevant portion of the Conley index theory in §3. Then in §4, we compute the connection matrices of the global attractors in each of the parameter regions, thereby obtaining algebraic data for the connecting orbit structures in each cases. These data are used to construct the semi-conjugacy model flows, which is carried out in §5. Finally we include a discussion concerning the main results and remaining problems.

We would like to thank P. Brunovský, X.-Y. Chen, and B. Fiedler for their useful comments and stimulating discussions.

2 Basic facts about the shadow system

In this section, we briefly summarize fundamental properties of the shadow system and its solutions, which play an important role in the following sections.

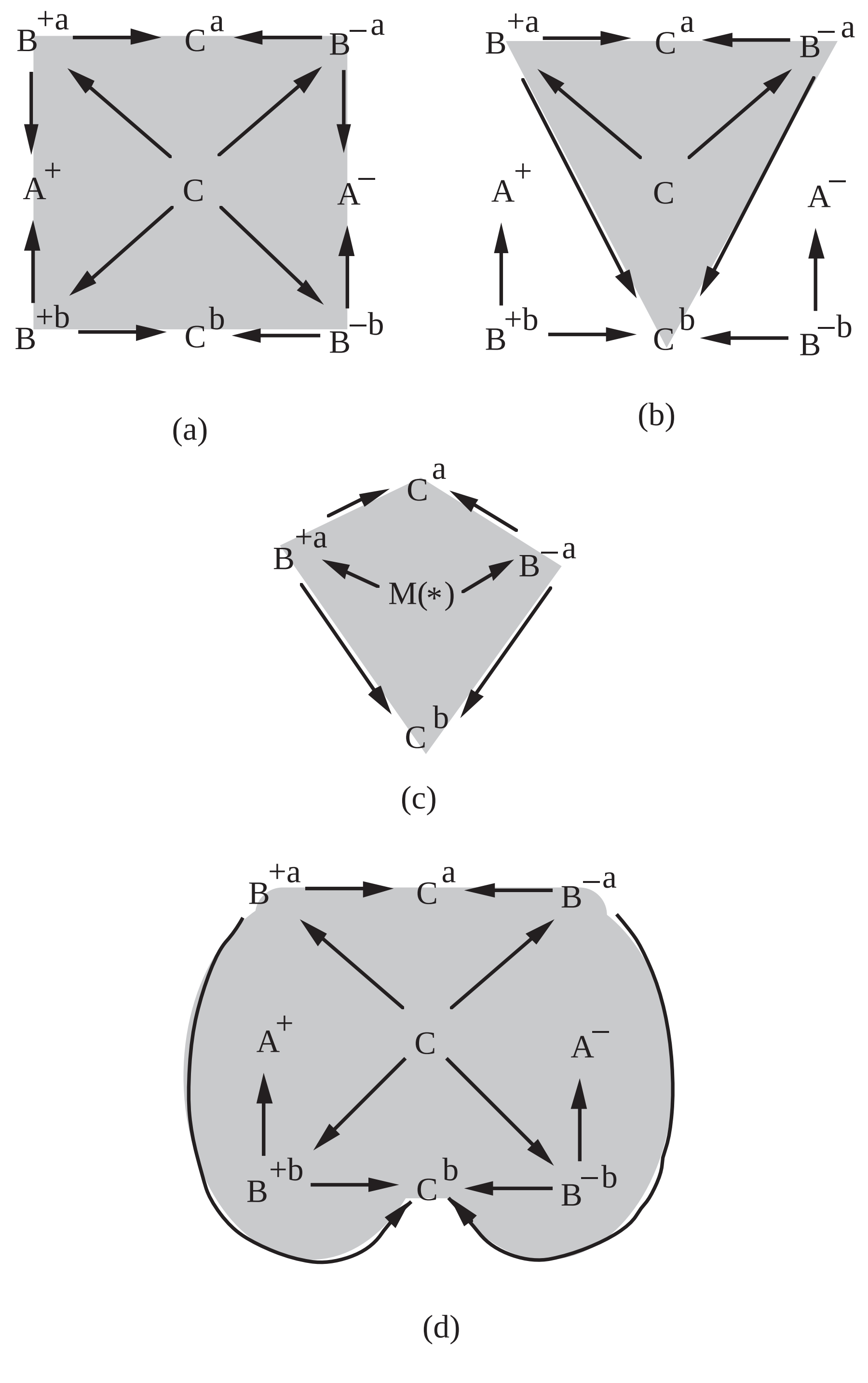

Figure 16: Three flows, to one of which $\mathcal{A}_{\mathcal{M}}(\mathrm{VIII}_+)$ is semi-conjugate.

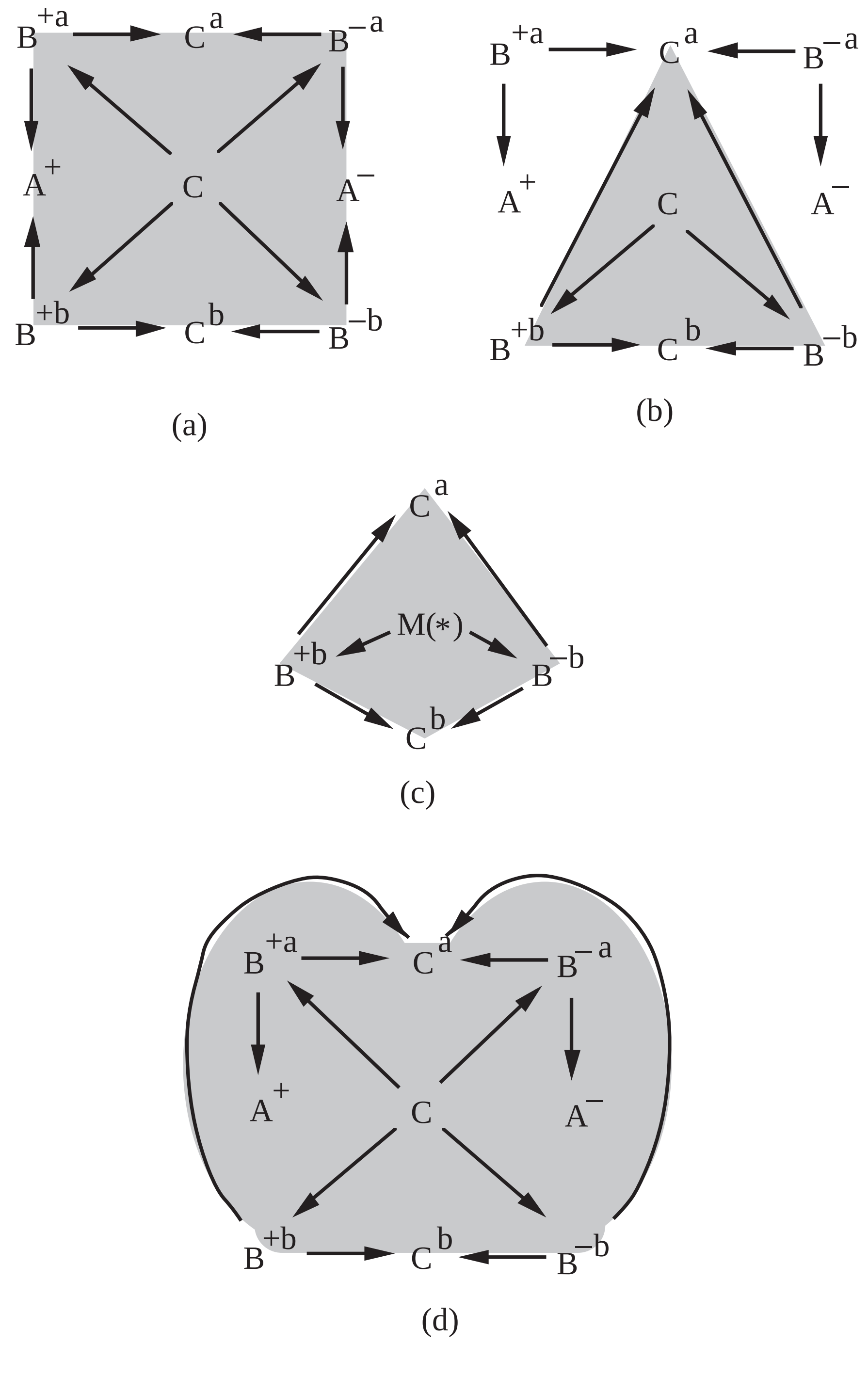

Figure 17: Three flows, to one of which $\mathcal{A}_{\mathcal{M}}(\mathrm{VIII}_-)$ is semi-conjugate.

2.1 The Lyapunov function for the shadow system

The shadow system is shown to be a gradient-like system ([8]).

Proposition 2.1 *If $\lambda \leq 1$, then the shadow system (1) admits a Lyapunov function*

$$L(u,\xi) = \int_I \left\{ \frac{\varepsilon^2}{2}|u_x|^2 - F(u) \right\} dx + \frac{1}{2\lambda}(\lambda\bar{u}+\mu)^2 + \frac{1}{2\lambda}(\lambda\bar{u}+\mu-\xi)^2$$

where $F(u) = \int f(u)du$ and $\bar{u} = \int_I u dx$. Namely, $L(u,\xi)$ decreases monotonically along an orbit as t increases.

Proof: Differentiate $L(u,\xi)$ with respect to t, then

$$\begin{aligned} \frac{dL}{dt} &= \int \varepsilon^2 u_x u_{xt} - f(u)u_t dx + (\lambda\bar{u}+\mu)\bar{u}_t + \frac{1}{\lambda}(\lambda\bar{u}+\mu-\xi)(\lambda\bar{u}_t - \xi_t) \\ &= -\int (\varepsilon^2 u_{xx} + f(u))u_t dx + 2(\lambda\bar{u}+\mu)\bar{u}_t - \xi\bar{u}_t - \frac{1}{\lambda}(\lambda\bar{u}+\mu-\xi)\xi_t \end{aligned}$$

using integration by parts together with the Neumann boundary condition. From the equation, we have

$$u_t = U - \xi, \quad \xi_t = \lambda\bar{u}+\mu-\xi$$

where $U = \varepsilon^2 u_{xx} + f(u)$, and hence

$$\begin{aligned} \frac{dL}{dt} &= -\int U(U-\xi)dx + 2(\lambda\bar{u}+\mu)\bar{u}_t - \xi\int(U-\xi)dx - \frac{1}{\lambda}(\lambda\bar{u}+\mu-\xi)^2 \\ &= -\int U^2 dx + 2(\lambda\bar{u}+\mu)\bar{u}_t - \xi^2 - \left(\frac{1}{\lambda}-1\right)(\lambda\bar{u}+\mu-\xi)^2 - (\lambda\bar{u}+\mu-\xi)^2 \\ &= -\int\{U^2 - 2(\lambda\bar{u}+\mu)U + (\lambda\bar{u}+\mu)^2\}dx - \left(\frac{1}{\lambda}-1\right)(\lambda\bar{u}+\mu-\xi)^2 \\ &= -\int\{U-(\lambda\bar{u}+\mu)\}^2 dx - \left(\frac{1}{\lambda}-1\right)(\lambda\bar{u}+\mu-\xi)^2 \quad \leq \quad 0, \end{aligned}$$

if $\lambda \leq 1$. This completes the proof. ∎

Remark 2.2 The condition $0 < k < 1$ is imposed in order that all the interesting bifurcations occur in the region $0 \leq \lambda \leq 1$ where the Lyapunov function is valid.

Let (u,ξ) be a stationary solution to the shadow system which depends on the parameters λ, μ, then the value of the Lyapunov function $L(u,\xi)$ can be thought of as a function of (λ,μ). The following proposition about the derivative with respect to the parameters turns out to be useful later.

Proposition 2.3 *For a family of stationary solution $(u,\xi)(\cdot\ ;\lambda,\mu)$ which depends on (λ,μ) smoothly, we have*

$$\frac{\partial}{\partial\mu}L((u,\xi)(\cdot\ ;\lambda,\mu)) = \frac{\xi}{\lambda} = \bar{u} + \frac{\mu}{\lambda}.$$

Proof: Since $(u,\xi)(\cdot\ ;\lambda,\mu)$ is a stationary solution, it satisfies

$$\varepsilon^2 u_{xx} + f(u) - \xi = 0, \quad \lambda\bar{u} + \mu - \xi = 0, \tag{4}$$

and hence

$$L(u,\xi) = \int \left(\frac{\varepsilon^2}{2}u_x^2 - F(u)\right) dx + \frac{\xi^2}{2\lambda}. \tag{5}$$

Differentiating it with respect to μ, we obtain

$$\begin{aligned}
\frac{\partial}{\partial\mu}L &= \int(\varepsilon^2 u_x u_{x\mu} - f(u)u_\mu)dx + \frac{\xi\xi_\mu}{\lambda} \\
&= -\int(\varepsilon^2 u_{xx} + f(u))u_\mu dx + \frac{\xi\xi_\mu}{\lambda} \\
&= -\int \xi u_\mu dx + \frac{\xi}{\lambda}(\lambda\bar{u}_\mu + 1) \\
&= \frac{\xi}{\lambda} \quad = \quad \bar{u} + \frac{\mu}{\lambda}.
\end{aligned}$$

■

2.2 Symmetry

The shadow system with Neumann zero boundary conditions possess a symmetry induced from the transformation of the solution by the inversion of the space variable: $x \mapsto -x$. Namely, if $(u(x,t),\xi(t))$ is a solution to the shadow system, then so is $(u(-x,t),\xi(t))$. We call this map $\gamma_N : (u(x,t),\xi(t)) \mapsto (u(-x,t),\xi(t))$ the Neumann symmetry. The Neumann symmetry flips the u-profile of a solution.

Furthermore, if $\mu = 0$, the nonlinearity (2) becomes odd symmetric so that, if $(u(x,t),\xi(t))$ is a solution to the shadow system, then so is $(-u(x,t),-\xi(t))$. This gives us another symmetry, and for convenience, we call $\gamma_O : (u(x,t),\xi(t)) \mapsto (-u(-x,t),\xi(t))$ the odd symmetry. The odd symmetry rotates the u-profile of a solution by 180°.

We have chosen the notation for stationary solutions in such a way that action of the symmetry transformations are easily seen, namely it is clear that the Neumann symmetry γ_N changes the sign of the superscript of the name for a steady solution, e.g. $\gamma_N(B^{+a}) = B^{-a}$. Similarly, the odd symmetry γ_O, when exists, changes the superscript 'a' into 'b' and vise versa, e.g. $\gamma_O(B^{+a}) = B^{+b}$. Moreover, since the Lyapunov function does not change under the symmetry transformations, its value should be preserved under these transformations.

2.3 Preservation of monotonicity

In the study of the connecting orbit structure for scalar parabolic partial differential equations, one of the key tool is the so-called the "lap number property" or "monotonicity of zero numbers" for solutions. Although the shadow system is not a scalar equation, it has analogous property as shown in the following proposition:

Proposition 2.4 *For a solution $(u(x,t), \xi(t))$, the number of zeros of the derivative $u_x(x,t)$ as a function of x is non-increasing as t increases.*

Proof: $w = u_x$ satisfies
$$w_t = \varepsilon^2 w_{xx} + f'(u)w$$
with $w = 0$ on ∂I. From [11] we have the desired conclusion. ∎

Corollary 2.5 *For any connecting orbit between monotone stationary solutions, the monotonicity is preserved, and hence a strictly increasing stationary solution cannot be connected with a strictly decreasing stationary solution and vise versa.*

2.4 Eigenvalues at spatially constant stationary solutions

In the following analysis, we sometimes need information about the eigenvalues at the spatially constant stationary solutions C, C^a, and C^b. Let (c, δ) be such a spatially constant stationary solution. The eigenvalue problem for (c, δ) is given by

$$\begin{aligned} \varepsilon^2 u_{xx} + (k - 3c^2)u - \xi &= \rho u, \\ \lambda \bar{u} - \xi &= \rho \xi, \end{aligned}$$

where ρ is an eigenvalue with the eigenfunction $(u, \xi) = (u(x), \xi)$. From the second equation, we eliminate ξ and obtain

$$\varepsilon^2 u_{xx} + (k - 3c^2 - \rho)u - \frac{\lambda}{1+\rho}\bar{u} = 0.$$

Integrating over the interval I using the Neumann boundary condition, we get

$$\left(k - 3c^2 - \rho - \frac{\lambda}{1+\rho}\right)\bar{u} = 0. \tag{6}$$

We have two cases: $\bar{u} = 0$ or $\bar{u} \neq 0$.

First we consider the case $\bar{u} = 0$. In this case we need to solve

$$\varepsilon^2 u_{xx} + (k - 3c^2 - \rho)u = 0.$$

Using the Neumann boundary condition, the solutions are given by

$$u = u_n(x) = \cos n\pi x$$

with the eigenvalues

$$\rho = \rho_n = k - 3c^2 - n^2\pi^2\varepsilon^2.$$

In particular, the largest eigenvalue among them is

$$\rho_1 = k - 3c^2 - \pi^2\varepsilon^2,$$

whose eigenfunction $(u_1(x), 0)$ lies in the space of monotone functions $\mathcal{M}$.

If $\bar{u} \neq 0$, then from (6) we have

$$k - 3c^2 - \rho - \frac{\lambda}{1+\rho} = 0,$$

or equivalently,

$$\rho^2 - (k - 3c^2 - 1)\rho - (k - 3c^2 - \lambda) = 0. \tag{7}$$

The discriminant of this quadratic equation is

$$D = (k - 3c^2 - 1)^2 + 4(k - 3c^2 - \lambda) = (k - 3c^2 + 1)^2 - 4\lambda.$$

Therefore, if $D \geq 0$, we have two real eigenvalues

$$\rho_0 = \frac{k - 3c^2 - 1 + \sqrt{D}}{2} \quad \text{and} \quad \rho_\infty = \frac{k - 3c^2 - 1 - \sqrt{D}}{2},$$

where $\rho_\infty < 0$. In fact, if $0 < \rho_\infty < \rho_0$, we have $1 < k - 3c^2 < \lambda$ which contradicts the assumption that $0 < \lambda \leq 1$.

From Proposition 1.1, we know that there are three distinct spatially constant stationary solutions C, C^a and C^b with $u_{C^b} < u_C < u_{C^a}$ for the parameter values in the regions $\mathrm{IV}_\pm$, $\mathrm{V}_\pm$, VI, $\mathrm{VII}_\pm$, VIII, where u_{C^b}, u_C, u_{C^a} stand for the u-component of C, C^a, C^b, respectively. Since the stationary solution (c, δ) is either C, C^a or C^b, which satisfies

$$kc - c^3 - \delta = 0, \qquad \lambda c + \mu - \delta = 0,$$

and hence,

$$c^3 - (k - \lambda)c + \mu = 0,$$

we must have

$$3c^2 - (k - \lambda) > 0$$

for $c = u_{C^a}$ or u_{C^b}, and

$$3c^2 - (k - \lambda) < 0$$

for $c = u_C$.

In the latter case, we have

$$D = (k - 3c^2 + 1)^2 - 4\lambda > (\lambda + 1)^2 - 4\lambda = (\lambda - 1)^2 > 0,$$

and hence we have two real eigenvalues $\rho_\infty < 0$ and ρ_0. Moreover $0 < \rho_0 < \rho_1$ for sufficiently small ε. In fact, $k - 3c^2 - \lambda > 0$ implies $\rho_0 > 0$, and $k - 3c^2 + 1 > \sqrt{D}$ for sufficiently small ε implies $\rho_1 > \rho_0$. In the former case, on the other hand, both roots of the quadratic equation (7) have a negative real part, since $k - 3c^2 - 1 < 0$. Note that, in the following analysis, we need information concerning the eigenvalues only when the stationary solution (c, δ) satisfies

$$-\sqrt{\frac{k}{3}} < c < \sqrt{\frac{k}{3}},$$

because, otherwise, $k - 3c^2 \le 0$ and hence all the eigenvalues $\rho_0, \rho_\infty, \rho_n$ for all n remain in the left half plane.

We summarize the results on eigenvalues at spatially constant stationary solutions.

Proposition 2.6 *In the parameter regions $IV_\pm$, $V_\pm$, VI, $VII_\pm$, VIII, the following holds for a spatially constant stationary solution (c, δ) satisfying $-\sqrt{k/3} < c < \sqrt{k/3}$:*

1. *For $c = u_{C^a}$ or u_{C^b}, the principal unstable eigenvalue is $\rho_1 = k - 3c^2 - \pi^2\varepsilon^2$ whose eigenfunction is monotone. The remaining unstable eigenvalues have non-monotone eigenfunctions.*

2. *For $c = u_C$, the principal unstable eigenvalue is $\rho_1 = k - 3c^2 - \pi^2\varepsilon^2$ whose eigenfunction is monotone. The remaining unstable eigenvalues have non-monotone eigenfunctions except $\rho_0 = \frac{k-3c^2-1+\sqrt{D}}{2}$ whose eigenfunction is constant.*

Corollary 2.7 *Under the same assumptions, there exists a one dimensional strong unstable manifold for C^a and C^b whose tangent space at the stationary solution is contained in the space of monotone functions $\mathcal{M}$. All orbits in the local unstable manifolds of C^a and C^b other than those in the strong stable manifolds are not entirely contained in $\mathcal{M}$.*

Proof: The first assertion is obvious because the strongest unstable eigenvalue ρ_1 has a monotone eigenfunction. Orbits in the local unstable manifolds are tangent to non-monotone eigendirections unless they are in the strong unstable manifolds. Therefore they cannot remain in $\mathcal{M}$. ∎

3 Conley index, connection matrix and transition matrix

We begin with a brief review of some of the relevant portions of the Conley index theory. Basic references for this material are [3, 1, 22, 23, 24].

Let $\varphi : \mathbf{R} \times X \to X$ be a flow on a locally compact topological space. In our case we will choose $X = \mathcal{A}_{\mathcal{M}}$. Let $N \subset X$ be a compact set. N is an *isolating neighborhood* if its maximal invariant set is contained strictly in its interior, i.e.

$$\mathrm{Inv}(N, \varphi) := \{x \in N \mid \varphi(\mathbf{R}, x) \subset N\} \subset \mathrm{int} N.$$

If $S = \mathrm{Inv}(N, \varphi)$ for some isolating neighborhood N, then S is called an isolated invariant set.

A *Morse decomposition* of an isolated invariant set S is a finite collection of disjoint compact invariant subsets of S,

$$\mathcal{M}(S) = \{M(p) \mid p \in \mathcal{P}\}$$

off of which one can define a Lyapunov function, i.e. there exists a continuous function $V : S \to \mathbf{R}$ such that if $u \notin \bigcup_{p\in\mathcal{P}} M(p)$ and $t > 0$, then $V(u) > V(\varphi(t, u))$. These individual invariant subsets, $M(p)$, are called *Morse sets*, and the remaining portion, $S \setminus \cup M(p)$, is referred to as the set of *connecting orbits.* In particular, given two Morse sets $M(p)$ and $M(q)$, the set of connecting orbits from $M(p)$ to $M(q)$ is defined to be

$$C(M(p), M(q)) := \{u \in S \mid \omega(u) \subset M(q),\ \alpha(u) \subset M(p)\}$$

where α and ω denote the *alpha* and *omega* limit sets, respectively. Because of the Lyapunov function, if $C(M(p), M(q)) \neq \emptyset$ then $C(M(q), M(p)) = \emptyset$. This implies that one can impose a partial order on the indexing set $\mathcal{P}$ by setting

$p > q$ if $C(M(p), M(q)) \neq \emptyset$, and taking the transitive closure. This order is called the *flow defined order* on $\mathcal{P}$.

If $\mathcal{M}(S) = \{M(p) \mid p \in \mathcal{P}\}$ is a Morse decomposition of S, then each $M(p)$ is an isolated invariant set. S contains other isolated invariant sets, some of which can be produced by the partial order on $\mathcal{P}$ as follows. A subset $I \subset \mathcal{P}$ is an *interval* in $\mathcal{P}$ if $r \in I$ whenever $p < r < q$ and $p, q \in I$. Disjoint intervals I and J are ordered $I < J$ if $i < j$ for every $i \in I, j \in J$. They are adjacent if $IJ = I \cup J$ is also an interval (i.e. if no element of $\mathcal{P}$ lies "between" I and J). If I is an interval, let

$$M(I) := \left(\bigcup_{i \in I} M(i) \right) \bigcup \left(\bigcup_{i,j \in I} C(M(j), M(i)) \right).$$

The simplest non-trivial Morse decomposition, is perhaps the most important. An *attractor repeller pair* in S consists of two sets (A, R) such that

1. A is an *attractor* in S, i.e. there is a positively invariant neighborhood U of A in S with $\omega(U) = A$.

2. R is the *dual repeller* to A in S, i.e. $R = S \setminus \{u | \omega(u) \subset (A)\}$.

Note that A and R are both isolated invariant sets, and if

$$C(R, A) = \{u \in S \mid \alpha(u) \subset R, \omega(u) \subset A\},$$

then $S = R \cup C(R, A) \cup A$. Observe that given a Morse decomposition and two adjacent intervals I and J in the indexing set with $I < J$, then $(M(I), M(J))$ is an attractor-repeller pair for $M(IJ)$.

The Conley index will be used to understand the structure of the dynamics of the maximal invariant set within an isolating neighborhood. Recall that the cohomological Conley index of an isolated invariant set S is defined in terms of an index pair (N, L) (see [3, 23, 1]), i.e.

$$CH^*(S) := H^*(N, L)$$

where the Alexander-Spanier cohomology with $\mathbf{Z}_2$ coefficients is used throughout this paper. The index is well defined since $CH^*(S)$ is independent of the index pair chosen.

In the case of isolated fixed points the following standard result will be used to determine the appropriate Conley index.

Proposition 3.1 *If p is a hyperbolic fixed point with unstable manifold of dimension n, then*

$$CH^k(p) \cong \begin{cases} \mathbf{Z}_2 & \textit{if } k = n, \\ 0 & \textit{otherwise.} \end{cases}$$

In an attractor-repeller decomposition, the Conley indices of the total invariant set, the attractor and the repeller are naturally related by an *index triple*. An index triple for an attractor-repeller pair (A, R) in S is a triple of compact spaces (N, M, L) such that (N, L) is an index pair for S, (N, M) is an index pair for R and (M, L) is an index pair for A. Such triples exist for any attractor-repeller decomposition. The cohomology exact sequence of the triple

$$\xrightarrow{\delta} H^k(N, M) \to H^k(N, L) \to H^k(M, L) \xrightarrow{\delta} H^{k+1}(N, M) \to$$

induces an exact sequence

$$\xrightarrow{\delta} CH^k(R) \to CH^k(S) \to CH^k(A) \xrightarrow{\delta} CH^{k+1}(R) \to$$

which is known as the cohomology attractor-repeller sequence. The boundary map δ is called the *connection map*, as $\delta \neq 0$ implies that connections between R and A exist.

All of these objects have generalizations to Morse decompositions. Index triples are generalized to index filtrations, and the attractor-repeller sequence is generalized to the construction of connection matrices. Recall that the *connection matrix* is a linear map defined on the graded modules made up of the sum of the cohomology indices of Morse sets in a Morse decomposition. In our case

$$\Delta : \bigoplus_{p \in \mathcal{P}} CH^*(M(p)) \to \bigoplus_{p \in \mathcal{P}} CH^*(M(p)).$$

Furthermore, connection matrices satisfy the following conditions.

1. They are *lower triangular*, i.e. if $p \not> q$ then

   $$0 = \Delta(q, p) : CH^*(M(q)) \to CH^*(M(p)).$$

2. They are *coboundary operators*, i.e. they are degree $+1$ maps

   $$\Delta(q, p) CH^n(M(q)) \subset CH^{n+1}(M(p)),$$

   and they square to zero, $\Delta \circ \Delta = 0$.

3. If p and q are adjacent in the flow defined order then the connection matrix entry $\Delta(q, p)$ equals the connecting homomorphism for the attractor repeller pair $(M(q), M(p))$ of $M(q, p)$.

4. The relation between the local cohomology indices, i.e. that of the Morse sets, and the global cohomology index is

   $$CH^*(S) \approx \frac{\ker \Delta}{\text{image} \Delta}.$$

The following theorem, due to Franzosa [5], is fundamental.

Theorem 3.2 *Given a Morse decomposition, there exists at least one connection matrix.*

Another result which we shall make frequent use of is the following.

Theorem 3.3 ([14, Corollary 3.3]) *Assume that $M(q)$ and $M(p)$ are hyperbolic equilibria whose stable and unstable manifolds intersect transversely. Furthermore, assume that $p > q$ are adjacent and that, for some n,*

$$CH^k(M(p)) \approx \begin{cases} \mathbf{Z_2} & \text{if } k = n+1, \\ 0 & \text{otherwise;} \end{cases} \qquad CH^k(M(q)) \approx \begin{cases} \mathbf{Z_2} & \text{if } k = n, \\ 0 & \text{otherwise.} \end{cases}$$

Then, using $\mathbf{Z}_2$ coefficients $\Delta(q,p)$ is given by the number of connecting orbits from $M(p)$ to $M(q)$ mod 2.

Now assume that the Morse decomposition continues over a connected region Λ in some compact parameter space (see [6]). Furthermore, assume that Δ_0 is a connection matrix at parameter value $\lambda_0 \in \Lambda$. Then, by [7], given $\lambda_1 \in \Lambda$, the corresponding connection matrix Δ_1 is given by

$$\Delta_1 = T^{-1} \circ \Delta_0 \circ T,$$

where the *algebraic transition matrix*

$$T : \bigoplus_{p \in \mathcal{P}} CH^*(M(p)) \to \bigoplus_{p \in \mathcal{P}} CH^*(M(p))$$

is a degree zero upper triangular isomorphism. Notice that this implies that

$$T(p,p) : CH^*(M(p)) \to CH^*(M(p))$$

is an isomorphism. In particular, the set of connection matrices over Λ is a subset of all matrices obtained by conjugating a known connection matrix by all possible algebraic transition matrices.

Another aspect of the index which we shall make use of is its behavior under semi-conjugacies (cf. [12, 13]). The essence of the matter is that the index theory is natural with respect to semi-conjugacies, as long as one works with pre-images, rather than images. A technicality is that the semi-conjugacy must be a *proper map*, i.e. pre-images of compact sets must be compact. Thus, if $\rho : X \to Y$ is a proper semi-conjugacy, and S an isolated invariant set in Y with index pair (N, L), then $T = \rho^{-1}(S)$ is an isolated invariant set in X with index pair $(\rho^{-1}(N), \rho^{-1}(L))$. Therefore, there is a map $\rho^* : CH^*(S) \to CH^*(T)$.

Similarly, if $\{M(p)\}$ is a Morse decomposition of S, then $\{T(p) = \rho^{-1}(M(p))\}$ is a Morse decomposition of T, and any admissible ordering on S gives an admissible ordering on T. Thus we can use the same ordering for both decompositions, and if I is an interval in that ordering, there is a map $CH^*(M(I)) \to CH^*(T(I))$. Moreover, the attractor-repeller sequence is natural: if I and J are adjacent intervals with $I < J$, then there is a commutative diagram

$$\begin{array}{ccccccc}
\xrightarrow{\delta} & CH^p(M(J)) & \to & CH^p(M(IJ)) & \to & CH^p(M(J)) & \to \\
& \downarrow \rho^* & & \downarrow \rho^* & & \downarrow \rho^* & \\
\xrightarrow{\delta} & CH^p(T(J)) & \to & CH^p(T(IJ)) & \to & CH^p(T(J)) & \to
\end{array}$$

4 Computation of connection matrices

In this section, we compute the connection matrices for the global attractors restricted to the monotone solution subspace in each of the parameter regions. The corresponding Morse decompositions are given by the steady states introduced in §1 and the connecting orbits between them. We begin with the computation of the total index for the global attractor in the monotone solution subspace. This result is a minor generalization of ([10, Theorem 6.2], [16, Corollary 3.2]).

Proposition 4.1 *For all parameter values*

$$CH^k(\mathcal{A}_{\mathcal{M}}) \equiv \begin{cases} \mathbf{Z}_2 & \text{if } k = 0, \\ 0 & \text{otherwise,} \end{cases}$$

where $\mathcal{A}_{\mathcal{M}}$ stands for the global attractor in the monotone solution subspace.

Proof: In view of the existence of the Lyapunov function, the semi-flow (Φ, X) generated by the shadow system has a global attractor $\mathcal{A}$. It is possible to show that the monotone solution space $\mathcal{M} \subset X$ is contractible. Indeed, if $f \in \mathcal{M}$, then $sf \in \mathcal{M}$ for all $s \in [0,1]$, and hence the homotopy $h : [0,1] \times \mathcal{M} \to \mathcal{M};\ (s,f) \mapsto sf$ gives the conclusion.

Notice that $\mathcal{A}_{\mathcal{M}} = \mathrm{Inv}(\mathcal{A} \cap \mathcal{M})$ is the global attractor for the restricted semi-flow $(\Phi_{|\mathcal{M}}, \mathcal{M})$. In fact, since $\mathcal{M}$ is closed, $\mathcal{A} \cap \mathcal{M}$ is compact. Therefore $\mathcal{A}_{\mathcal{M}}$ is also compact. It is easy to see that $\mathcal{A}_{\mathcal{M}}$ is a global attractor from the definition and the positive invariance of $\mathcal{M}$ under the semi-flow Φ.

Now take a ball $B \subset X$ with a sufficiently large radius, then $B \cap \mathcal{M}$ is contractible in $\mathcal{M}$ from (1). On the other hand, $B \cap \mathcal{M}$ is homotopic to $\mathcal{A}_{\mathcal{M}}$ with the flow-defined homotopy. Therefore, we conclude that

$$CH^k(\mathcal{A}_{\mathcal{M}}) \equiv CH^k(B \cap \mathcal{M}) \equiv CH^k(\mathrm{pt}) \equiv \begin{cases} \mathbf{Z}_2 & \text{if } k = 0, \\ 0 & \text{otherwise.} \end{cases}$$

■

Proposition 4.2 (connection matrix for I) *In region I, the connection matrix is uniquely given as follows:*

$$\Delta(\mathrm{I}) = \begin{array}{c} A^+ \\ A^- \\ C \end{array} \begin{pmatrix} & & \\ \multicolumn{2}{c}{\text{\Large 0}} & \text{\Large 0} \\ 1 \;\; 1 & & 0 \end{pmatrix}.$$

Proof: From the symmetry, we can put the connection matrix in the following form:

$$\Delta(\mathrm{I}) = \begin{pmatrix} & & \\ \multicolumn{2}{c}{\text{\Large 0}} & \text{\Large 0} \\ a \;\; a & & 0 \end{pmatrix}.$$

Since $\mathrm{rank}\Delta(\mathrm{I}) = 1$, we have $a = 1$. ■

Proposition 4.3 (connection matrix for II_+) *In region II_+, the connection matrix is uniquely given as follows:*

$$\Delta(\mathrm{II}_+) = \begin{array}{c} C^b \\ A^+ \\ A^- \\ B^{+b} \\ B^{-b} \end{array} \begin{pmatrix} & & & \\ \multicolumn{3}{c}{\text{\Large 0}} & \text{\Large 0} \\ & & & \\ 1 & 1 & 0 & \\ 1 & 0 & 1 & \text{\Large 0} \end{pmatrix}.$$

Proof: From the symmetry and the preservation of monotonicity, we can put the connection matrix $\Delta(\mathrm{II}_+)$ in the following form:

$$\Delta(\mathrm{II}_+) = \begin{array}{c} C^b \\ A^+ \\ A^- \\ B^{+b} \\ B^{-b} \end{array} \begin{pmatrix} & & & \\ \multicolumn{3}{c}{\text{\Large 0}} & \text{\Large 0} \\ & & & \\ a & b & 0 & \\ a & 0 & b & \text{\Large 0} \end{pmatrix}.$$

Since $\mathrm{rank}\Delta(\mathrm{II}_+) = 2$, we have $b = 1$, and since $\dim W^u(B^{\pm b}) = 1$, the branch of $W^u(B^{\pm b})$ not connecting to $A^{\pm}$ must connect to C^b due to Theorem 3.3, and hence $a = 1$. ■

Remark: This result was obtained by [8] for the first time.

A similar argument also works for the connection matrix in region II_- and we get the following proposition.

Proposition 4.4 (connection matrix for II_-) *In region* II_-*, the connection matrix is uniquely given as follows:*

$$\Delta(\mathrm{II}_-) = \begin{array}{c} C^a \\ A^+ \\ A^- \\ B^{+a} \\ B^{-a} \end{array} \left(\begin{array}{ccc|c} & \mathbf{0} & & \mathbf{0} \\ & & & \\ & & & \\ 1 & 1 & 0 & \mathbf{0} \\ 1 & 0 & 1 & \end{array} \right).$$

The connection matrices in the regions $\mathrm{III}_\pm$ are trivially zero since there is a unique stable equilibrium point C^b or C^a, respectively.

Proposition 4.5 (connection matrix for IV_+) *In region* IV_+*, the connection matrix is uniquely given as follows:*

$$\Delta(\mathrm{IV}_+) = \begin{array}{c} C^b \\ C^a \\ C \end{array} \begin{pmatrix} 0 & 0 & 0 \\ 0 & 0 & 0 \\ 0 & 1 & 0 \end{pmatrix}.$$

Proof: Since the connection matrix is a degree $+1$ map, it takes the form

$$\Delta(\mathrm{IV}_+) = \begin{array}{c} C^b \\ C^a \\ C \end{array} \begin{pmatrix} 0 & 0 & 0 \\ a & 0 & 0 \\ 0 & b & 0 \end{pmatrix}.$$

Since C^a has a one dimensional unstable manifold restricted to $\mathcal{A}_\mathcal{M}$ (Corollary 2.7) whose branches must be connected to C^b, we have $a = 0$. Then, from $\mathrm{rank}\Delta(\mathrm{IV}_+) = 1$, we get $b = 1$. Note that $a = 0$ indicates a double connection from C^a to C^b (Theorem 3.3), which is persistent under perturbation even at the boundary $\mu \approx \sqrt{k}\lambda$ where a saddle-node bifurcation occurs unrelated to the equilibria C^a and C^b. ∎

Similarly, we obtain

Proposition 4.6 (connection matrix for IV_-) *In region* IV_-*, the connection matrix is uniquely given as follows:*

$$\Delta(\mathrm{IV}_-) = \begin{array}{c} C^a \\ C^b \\ C \end{array} \begin{pmatrix} 0 & 0 & 0 \\ 0 & 0 & 0 \\ 0 & 1 & 0 \end{pmatrix}.$$

Proposition 4.7 (connection matrix for V_+**)** *In region* V_+*, the connection matrix is uniquely given as follows:*

$$\Delta(\mathrm{V}_+) = \begin{array}{c} C^a \\ C^b \\ B^{+a} \\ B^{-a} \\ C \end{array} \left(\begin{array}{ccccc} \multicolumn{2}{c}{0} & \multicolumn{2}{c}{0} & 0 \\ & & & & \\ 1 & 1 & \multicolumn{2}{c}{0} & 0 \\ 1 & 1 & & & \\ \multicolumn{2}{c}{0} & 1 & 1 & 0 \end{array}\right).$$

Proof: From the Neumann symmetry, the connection matrix takes the form

$$\Delta(\mathrm{V}_+) = \begin{array}{c} C^a \\ C^b \\ B^{+a} \\ B^{-a} \\ C \end{array} \left(\begin{array}{ccccc} \multicolumn{2}{c}{0} & \multicolumn{2}{c}{0} & 0 \\ & & & & \\ a & b & \multicolumn{2}{c}{0} & 0 \\ a & b & & & \\ \multicolumn{2}{c}{0} & c & c & 0 \end{array}\right).$$

From $\mathrm{rank}\Delta(\mathrm{V}_+) = 2$, we have $c = 1$ and either a or b is not zero. Using $\dim W^u(B^{\pm a}) = 1$, we conclude $a = b = 1$. ■

Similarly we have

Proposition 4.8 (connection matrix for V_-**)** *In region* V_-*, the connection matrix is uniquely given as follows:*

$$\Delta(\mathrm{V}_-) = \begin{array}{c} C^a \\ C^b \\ B^{+b} \\ B^{-b} \\ C \end{array} \left(\begin{array}{ccccc} \multicolumn{2}{c}{0} & \multicolumn{2}{c}{0} & 0 \\ & & & & \\ 1 & 1 & \multicolumn{2}{c}{0} & 0 \\ 1 & 1 & & & \\ \multicolumn{2}{c}{0} & 1 & 1 & 0 \end{array}\right).$$

Proposition 4.9 (connection matrix for VI**)** *In region* VI*, the connection matrix is uniquely given as follows:*

$$\Delta(\mathrm{VI}) = \begin{array}{c} A^+ \\ A^- \\ C^a \\ C^b \\ C \end{array} \left(\begin{array}{ccccc} \multicolumn{2}{c}{0} & \multicolumn{2}{c}{0} & 0 \\ & & & & \\ 1 & 1 & \multicolumn{2}{c}{0} & 0 \\ 1 & 1 & & & \\ \multicolumn{2}{c}{0} & 1 & 1 & 0 \end{array}\right).$$

Proof: From the Neumann symmetry, the connection matrix takes the form

$$\Delta(\mathrm{VI}) = \begin{array}{c} A^+ \\ A^- \\ C^a \\ C^b \\ C \end{array} \left(\begin{array}{ccccc} \multicolumn{2}{c}{0} & \multicolumn{2}{c}{0} & 0 \\ & & & & \\ a & a & \multicolumn{2}{c}{0} & 0 \\ b & b & & & \\ \multicolumn{2}{c}{0} & c & d & 0 \end{array}\right).$$

Since $\mathrm{rank}\Delta(\mathrm{VI}) = 2$, either a or b is not zero and either c or d is not zero. If $a = 0$, then there must exist either no connection or 4 connections in $\mathcal{A}_{\mathcal{M}}$ from C^a to $A^{\pm}$, but this is absurd because there are two and only two branches of the unstable manifold of C^a restricted to $\mathcal{A}_{\mathcal{M}}$ (Corollary 2.7). Therefore $a = 1$. Similarly $b = 1$. From $\Delta(\mathrm{VI})^2 = 0$, we have $ac + bd = c + d = 0$, and hence $c = d = 1$. ∎

Proposition 4.10 (connection matrix for VII_+**)** *The set of possible connection matrices over the region* VII_+ *contains the following two matrices:*

$$\Delta(\mathrm{VII}_+)_1 = \begin{array}{c} C^b \\ A^+ \\ A^- \\ C^a \\ B^{+b} \\ B^{-b} \\ C \end{array} \begin{pmatrix} 0 & 0 & 0 & 0 & 0 & 0 & 0 \\ 0 & 0 & 0 & 0 & 0 & 0 & 0 \\ 0 & 0 & 0 & 0 & 0 & 0 & 0 \\ 0 & 1 & 1 & 0 & 0 & 0 & 0 \\ 1 & 1 & 0 & 0 & 0 & 0 & 0 \\ 1 & 0 & 1 & 0 & 0 & 0 & 0 \\ 0 & 0 & 0 & 1 & 1 & 1 & 0 \end{pmatrix};$$

$$\Delta(\mathrm{VII}_+)_2 = \begin{array}{c} C^b \\ A^+ \\ A^- \\ C^a \\ B^{+b} \\ B^{-b} \\ C \end{array} \begin{pmatrix} 0 & 0 & 0 & 0 & 0 & 0 & 0 \\ 0 & 0 & 0 & 0 & 0 & 0 & 0 \\ 0 & 0 & 0 & 0 & 0 & 0 & 0 \\ 0 & 0 & 0 & 0 & 0 & 0 & 0 \\ 1 & 1 & 0 & 0 & 0 & 0 & 0 \\ 1 & 0 & 1 & 0 & 0 & 0 & 0 \\ 0 & 0 & 0 & 1 & 0 & 0 & 0 \end{pmatrix}.$$

The corresponding transition matrix between these two connection matrices is

$$T(\mathrm{VII}_+) = \begin{array}{c} C^b \\ A^+ \\ A^- \\ C^a \\ B^{+b} \\ B^{-b} \\ C \end{array} \begin{pmatrix} 1 & 0 & 0 & 0 & 0 & 0 & 0 \\ 0 & 1 & 0 & 0 & 0 & 0 & 0 \\ 0 & 0 & 1 & 0 & 0 & 0 & 0 \\ 0 & 0 & 0 & 1 & 1 & 1 & 0 \\ 0 & 0 & 0 & 0 & 1 & 0 & 0 \\ 0 & 0 & 0 & 0 & 0 & 1 & 0 \\ 0 & 0 & 0 & 0 & 0 & 0 & 1 \end{pmatrix}.$$

If $T(\mathrm{VII}_+)$ *is realized, this indicates the existence of a global bifurcation corresponding to the saddle-saddle connection between* C^a *and* $B^{\pm b}$*.*

Proof: The symmetry as well as the preservation of the monotonicity assumes the connection matrix in the following form:

$$\Delta(\mathrm{VII}_+) = \begin{array}{c} C^b \\ A^+ \\ A^- \\ C^a \\ B^{+b} \\ B^{-b} \\ C \end{array} \left(\begin{array}{ccccccc} & & & & & & \\ & \mathbf{0} & & & \mathbf{0} & & \mathbf{0} \\ & & & & & & \\ l & n & n & & & & \\ m & p & 0 & & \mathbf{0} & & \mathbf{0} \\ m & 0 & p & & & & \\ & 0 & & q & r & r & 0 \end{array}\right). \tag{8}$$

In particular, just after the pitchfork bifurcation from the region VI to the region VII_+, the corresponding connection matrix $\Delta_{\mathrm{VI}}(\mathrm{VII})$ takes the form $\Delta(\mathrm{VII}_+)_1$ as above.

The transition matrix between these two is given by

$$T(\mathrm{VII}_+) = \begin{array}{c} C^b \\ A^+ \\ A^- \\ C^a \\ B^{+b} \\ B^{-b} \\ C \end{array} \left(\begin{array}{ccccccc} 1 & 0 & 0 & & & & \\ 0 & 1 & 0 & & \mathbf{0} & & \mathbf{0} \\ 0 & 0 & 1 & & & & \\ & & & y & z & z & \\ & \mathbf{0} & & w & x & 0 & \mathbf{0} \\ & & & w & 0 & x & \\ & 0 & & & 0 & & 1 \end{array}\right),$$

and the invertibility yields $yx^2 \neq 0$, hence $x = y = 1$.

Due to [7], we only need to consider upper-triangular transition matrices which in our case are given by either $z = 0$ or $w = 0$. However $z = 0,\ w = 1$ is not the case, because, from the relation

$$\Delta(\mathrm{VII}_+) = T(\mathrm{VII}_+)^{-1} \circ \Delta(\mathrm{VII}_+)_1 \circ T(\mathrm{VII}_+),$$

the resulting connection matrix cannot be of the general form given in (8). For the case of $z = 1,\ w = 0$, on the other hand, we have the form $\Delta(\mathrm{VII}_+)_2$ by the same reasoning. ■

Again, the same argument concludes the following proposition:

Proposition 4.11 (connection matrix for VII_-**)** *The set of possible connection matrices over the region* VII_- *contains the following two matrices:*

$$\Delta(\mathrm{VII}_-)_1 = \begin{array}{c} C^a \\ A^+ \\ A^- \\ C^b \\ B^{+a} \\ B^{-a} \\ C \end{array} \left(\begin{array}{ccccccc} & & & & & & \\ & \mathbf{0} & & & \mathbf{0} & & \mathbf{0} \\ & & & & & & \\ 0 & 1 & 1 & & & & \\ 1 & 1 & 0 & & \mathbf{0} & & \mathbf{0} \\ 1 & 0 & 1 & & & & \\ & 0 & & 1 & 1 & 1 & 0 \end{array}\right);$$

$$\Delta(\mathrm{VII}_-)_2 = \begin{array}{c} C^a \\ A^+ \\ A^- \\ C^b \\ B^{+a} \\ B^{-a} \\ C \end{array} \left(\begin{array}{ccccccc} & & & & & & \\ \multicolumn{3}{c}{\mathbf{0}} & \multicolumn{3}{c}{\mathbf{0}} & \mathbf{0} \\ & & & & & & \\ 0 & 0 & 0 & & & & \\ 1 & 1 & 0 & \multicolumn{3}{c}{\mathbf{0}} & \mathbf{0} \\ 1 & 0 & 1 & & & & \\ \multicolumn{3}{c}{0} & 1 & 0 & 0 & 0 \end{array} \right).$$

The corresponding transition matrix between these two connection matrices is

$$T(\mathrm{VII}_-) = \begin{array}{c} C^a \\ A^+ \\ A^- \\ C^b \\ B^{+a} \\ B^{-a} \\ C \end{array} \left(\begin{array}{ccccccc} 1 & 0 & 0 & & & & \\ 0 & 1 & 0 & \multicolumn{3}{c}{\mathbf{0}} & \mathbf{0} \\ 0 & 0 & 1 & & & & \\ & & & 1 & 1 & 1 & \\ \multicolumn{3}{c}{\mathbf{0}} & 0 & 1 & 0 & \mathbf{0} \\ & & & 0 & 0 & 1 & \\ \multicolumn{3}{c}{0} & \multicolumn{3}{c}{0} & 1 \end{array} \right).$$

If $T(\mathrm{VII}_-)$ is realized, this indicates the existence of a global bifurcation corresponding to the saddle-saddle connection between C^b and $B^{\pm a}$.

Proposition 4.12 (connection matrix for VIII)
(i) The connection matrix for the region VIII_0 is uniquely given by

$$\Delta(\mathrm{VIII})_1 = \begin{array}{c} C^a \\ C^b \\ A^+ \\ A^- \\ B^{+a} \\ B^{+b} \\ B^{-a} \\ B^{-b} \\ C \end{array} \left(\begin{array}{ccccccccc} & & & & & & & & \\ & & & & & & & & \\ \multicolumn{4}{c}{\mathbf{0}} & \multicolumn{4}{c}{\mathbf{0}} & \mathbf{0} \\ & & & & & & & & \\ 1 & 0 & 1 & 0 & & & & & \\ 0 & 1 & 1 & 0 & \multicolumn{4}{c}{\mathbf{0}} & \mathbf{0} \\ 1 & 0 & 0 & 1 & & & & & \\ 0 & 1 & 0 & 1 & & & & & \\ \multicolumn{4}{c}{0} & 1 & 1 & 1 & 1 & 0 \end{array} \right).$$

(ii) The set of possible connection matrices over the region VIII_+ *contains the following two matrices:*

$$\Delta(\mathrm{VIII})_1 = \quad \begin{array}{c} C^a \\ C^b \\ A^+ \\ A^- \\ B^{+a} \\ B^{+b} \\ B^{-a} \\ B^{-b} \\ C \end{array} \left(\begin{array}{ccccccccc} & & & & & & & & \\ & & & & & & & & \\ & \mathbf{0} & & & & \mathbf{0} & & & \mathbf{0} \\ & & & & & & & & \\ 1 & 0 & 1 & 0 & & & & & \\ 0 & 1 & 1 & 0 & & \mathbf{0} & & & \mathbf{0} \\ 1 & 0 & 0 & 1 & & & & & \\ 0 & 1 & 0 & 1 & & & & & \\ & 0 & & & 1 & 1 & 1 & 1 & 0 \end{array}\right);$$

$$\Delta(\mathrm{VIII})_2 = \quad \begin{array}{c} C^a \\ C^b \\ A^+ \\ A^- \\ B^{+a} \\ B^{+b} \\ B^{-a} \\ B^{-b} \\ C \end{array} \left(\begin{array}{ccccccccc} & & & & & & & & \\ & & & & & & & & \\ & \mathbf{0} & & & & \mathbf{0} & & & \mathbf{0} \\ & & & & & & & & \\ 1 & 1 & 0 & 0 & & & & & \\ 0 & 1 & 1 & 0 & & \mathbf{0} & & & \mathbf{0} \\ 1 & 1 & 0 & 0 & & & & & \\ 0 & 1 & 0 & 1 & & & & & \\ & 0 & & & 1 & 0 & 1 & 0 & 0 \end{array}\right).$$

In particular, there may exist a global bifurcation corresponding to the saddle-saddle connection between $B^{\pm a}$ *and* $B^{\pm b}$*, respectively, in transition between these two types of connecting orbit structures.*
(iii) The set of possible connection matrices over the region VIII_- *contains the following two matrices:*

$$\Delta(\mathrm{VIII})_1 = \quad \begin{array}{c} C^a \\ C^b \\ A^+ \\ A^- \\ B^{+a} \\ B^{+b} \\ B^{-a} \\ B^{-b} \\ C \end{array} \left(\begin{array}{ccccccccc} & & & & & & & & \\ & & & & & & & & \\ & \mathbf{0} & & & & \mathbf{0} & & & \mathbf{0} \\ & & & & & & & & \\ 1 & 0 & 1 & 0 & & & & & \\ 0 & 1 & 1 & 0 & & \mathbf{0} & & & \mathbf{0} \\ 1 & 0 & 0 & 1 & & & & & \\ 0 & 1 & 0 & 1 & & & & & \\ & 0 & & & 1 & 1 & 1 & 1 & 0 \end{array}\right);$$

$$
\Delta(\mathrm{VIII})_3 = \begin{array}{c} C^a \\ C^b \\ A^+ \\ A^- \\ B^{+a} \\ B^{+b} \\ B^{-a} \\ B^{-b} \\ C \end{array}
\left(\begin{array}{cccc|cccc|c}
 & & & & & & & & \\
 & & & & & & & & \\
 & \mathbf{0} & & & & \mathbf{0} & & & \mathbf{0} \\
 & & & & & & & & \\
0 & 1 & 1 & 0 & & & & & \\
1 & 1 & 0 & 0 & & \mathbf{0} & & & \mathbf{0} \\
0 & 1 & 0 & 1 & & & & & \\
1 & 1 & 0 & 0 & & & & & \\
 & 0 & & & 0 & 1 & 0 & 1 & 0
\end{array}\right).
$$

In particular, there may exist a global bifurcation corresponding to the saddle-saddle connection between $B^{\pm a}$ and $B^{\pm b}$, respectively.

Proof: (i) The symmetry and the preservation of monotonicity imply

$$
\Delta(\mathrm{VIII}) = \begin{array}{c} C^a \\ C^b \\ A^+ \\ A^- \\ B^{+a} \\ B^{+b} \\ B^{-a} \\ B^{-b} \\ C \end{array}
\left(\begin{array}{cccc|cccc|c}
 & & & & & & & & \\
 & & & & & & & & \\
 & \mathbf{0} & & & & \mathbf{0} & & & \mathbf{0} \\
 & & & & & & & & \\
a & c & e & 0 & & & & & \\
b & d & f & 0 & & \mathbf{0} & & & \mathbf{0} \\
a & c & 0 & e & & & & & \\
b & d & 0 & f & & & & & \\
 & 0 & & & l & m & l & m & 0
\end{array}\right).
$$

In particular, when $\mu = 0$, it admits the odd symmetry which implies that $\Delta(\mathrm{VIII})$ satisfies

$$a = d,\ b = c,\ e = f,\ l = m.$$

This together with $\mathrm{rank}\Delta(\mathrm{VIII}_0) = 4$ and

$$
\mathrm{rank}\begin{pmatrix} a & c & e & 0 \\ b & d & f & 0 \\ a & c & 0 & e \\ b & d & 0 & f \end{pmatrix} \le 3
$$

show that $e = 1,\ a \neq b,\ l \neq 0$ and hence $b = a + 1,\ l = 1$.

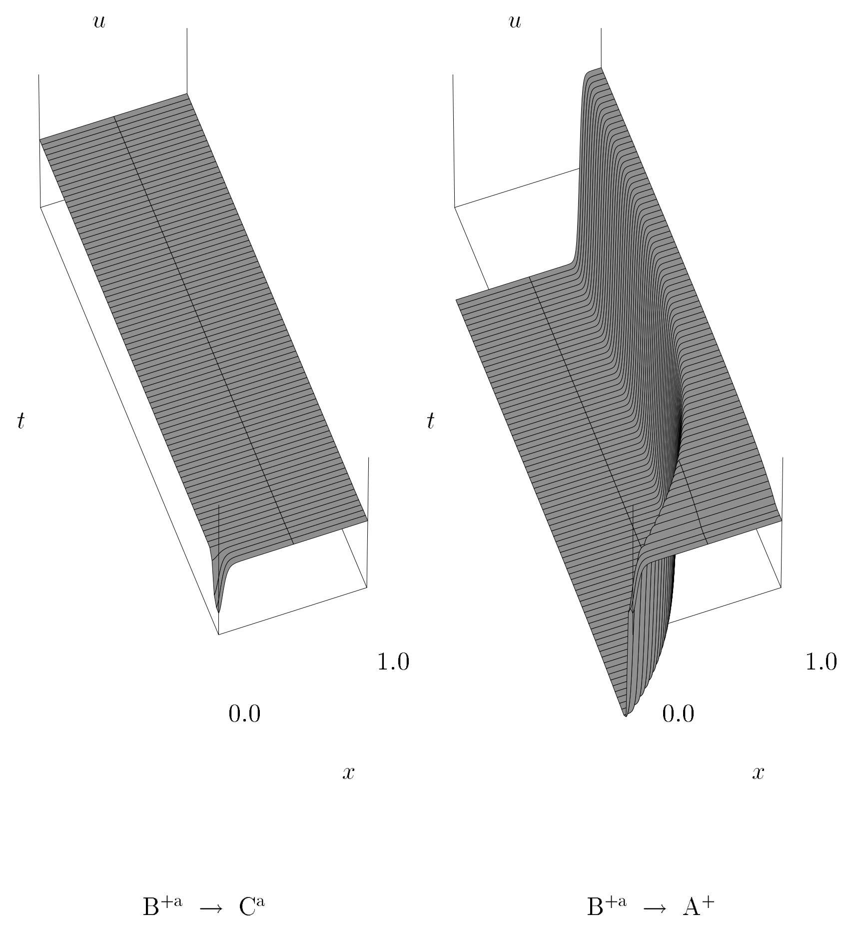

Figure 18: Numerical evidence for $a = 1$: connections $B^{+a} \to C^a$ and $B^{+a} \to A^+$. The parameter values are $k = 0.5,\ \varepsilon = 0.01,\ \lambda = 0.12$ and $\mu = 0.06$.

Due to the odd symmetry present in the region VIII_0, the transition matrix takes the following form:

$$T(\mathrm{VIII}) = \begin{array}{c} C^a \\ C^b \\ A^+ \\ A^- \\ B^{+a} \\ B^{+b} \\ B^{-a} \\ B^{-b} \\ C \end{array} \left(\begin{array}{ccccccccc} 1 & 0 & 0 & 0 & & & & & \\ 0 & 1 & 0 & 0 & & \mathbf{0} & & & \mathbf{0} \\ 0 & 0 & 1 & 0 & & & & & \\ 0 & 0 & 0 & 1 & & & & & \\ & & & & x & y & \mathbf{0} & & \\ & \mathbf{0} & & & y & x & & & \mathbf{0} \\ & & & & \mathbf{0} & & x & y & \\ & & & & & & y & x & \\ & 0 & & & & 0 & & & 1 \end{array} \right).$$

Since $L(B^{\pm a}) = L(B^{\pm b})$ in this region, we have $y = 0$ and hence $T(\mathrm{VIII}) = I$. In particular, the transition matrix is unique in VIII_0, which shows that the connecting orbit structure is robust in this region. Thus it is possible to determine the connection corresponding to the entry a in $\Delta(\mathrm{VIII})$ through numerical simulation. Take any parameter value from the region VIII_0, say $\lambda = 0.12$, $\mu = 0.0$. From the above computation of the connection matrix, we know that there exists a connecting orbit from B^{+a} to A^+. We are interested in finding a connection from B^{+a} to either C^a or C^b, which determines either $a = 1$ or $a = 0$. Since the steady states C^a and C^b are well distinguished, we can check it by following a branch of the 1-dimensional unstable manifold of B^{+a}. This is carried out and the result is exhibited in Figure 18, from which it is clear that there exists a $B^{+a} \to C^a$ connection, thereby proving $a = 1$. Therefore we have

$$\Delta(\mathrm{VIII})_1 = \begin{array}{c} C^a \\ C^b \\ A^+ \\ A^- \\ B^{+a} \\ B^{+b} \\ B^{-a} \\ B^{-b} \\ C \end{array} \left(\begin{array}{ccccccccc} & & & & & & & & \\ & & & & & & & & \\ & \mathbf{0} & & & & \mathbf{0} & & & \mathbf{0} \\ & & & & & & & & \\ 1 & 0 & 1 & 0 & & & & & \\ 0 & 1 & 1 & 0 & & \mathbf{0} & & & \mathbf{0} \\ 1 & 0 & 0 & 1 & & & & & \\ 0 & 1 & 0 & 1 & & & & & \\ & 0 & & & 1 & 1 & 1 & 1 & 0 \end{array} \right),$$

which proves the statement (i).

(ii) Without the odd symmetry present in the region VIII_0, the transition matrix can take the form

$$
T(\mathrm{VIII}) = \begin{array}{c} C^a \\ C^b \\ A^+ \\ A^- \\ B^{+a} \\ B^{+b} \\ B^{-a} \\ B^{-b} \\ C \end{array}
\left(\begin{array}{cccccccccc}
1 & 0 & 0 & 0 & & & & & \\
0 & 1 & 0 & 0 & & \mathbf{0} & & & \mathbf{0} \\
0 & 0 & 1 & 0 & & & & & \\
0 & 0 & 0 & 1 & & & & & \\
 & & & & x & z & \mathbf{0} & & \\
 & \mathbf{0} & & & w & y & & & \mathbf{0} \\
 & & & & \mathbf{0} & & x & z & \\
 & & & & & & w & y & \\
 & 0 & & & & 0 & & & 1
\end{array}\right).
$$

In the region VIII_+, it turns out that $L(B^{+a}) > L(B^{+b})$ since we observe that $L(B^{+a}) = L(B^{+b})$ on the line VIII_0 and that $\frac{\partial}{\partial\mu}\{L(B^{+a}) - L(B^{+b})\} > 0$ from Proposition 2.3. Therefore in the region VIII_+, the non-trivial algebraic transition matrix is given by $z = 1$ and $w = 0$, which implies that only $\Delta(\mathrm{VIII})_1$ and $\Delta(\mathrm{VIII})_2$ may occur.

(iii) Similarly in the region VIII_-, the transition matrix can take $z = 0$ and $w = 1$, and hence $\Delta(\mathrm{VIII})_1$ and $\Delta(\mathrm{VIII})_3$ are possible. ∎

5 Semi-conjugacies

The connection matrices computed in the previous section provide us with knowledge concerning the existence of connecting orbits between critical points whose index differ by degree one. In this section this information will be used to obtain semi-conjugacies from the dynamics of the shadow system onto the simple planar dynamical systems indicated in the Introduction. The approach is to separate the problem into two steps. The first involves construction of the map which provides the semi-conjugacy and is analytical in nature. The second step is to show that the map is onto and requires the algebraic topological machinery associated with the Conley index.

To begin with observe that the proof of Theorem 1.3 is elementary; the connection matrix indicates all possible connecting orbits and a straightforward argument (see [17, Theorem 2.2]) produces the semi-conjugacy. Theorem 1.4 follows from the analysis of the steady state solutions and the existence of the Lyapunov function discussed in the introduction. Theorems 1.6 and 1.7 follow from [17, Theorem 1.2]. Therefore, all that remains to be demonstrated are Theorems 1.5, 1.8, and 1.9. As will become clear at the end of this section, the proofs are quite similar in nature and thus it is worth starting with an abstract construction which can be applied to all cases.

5.1 General Constructions of the Semi-conjugacies

Let S be an isolated invariant set with a Morse decomposition and flow defined order

$$\mathcal{M}(S) = \{M(p) \mid p = 0, 1, 2,\ 2 > 1 > 0\}. \tag{9}$$

Observe that the set of non-trivial attractor repeller pair decompositions of S consist of

$$\begin{aligned} (A_0, R_0) &= (M(0), M(1,2)) \\ (A_1, R_1) &= (M(0,1), M(2)) \end{aligned}$$

The following proposition is a special case of Conley's decomposition theorem [3]

Proposition 5.1 *There exists a continuous Lyapunov function $V : S \to [0,2]$ such that $M(p) \subset V^{-1}(p)$, $p = 0, 1, 2$.*

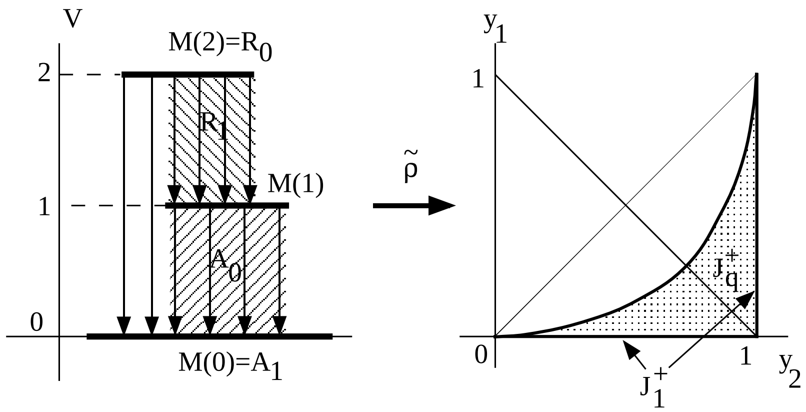

Figure 19: Map from the Morse decomposition onto $\mathcal{D}$.

For $i = 0, 1$, define functions $\tau_i : S \setminus (A_i \cup R_i) \to \mathbf{R}$ by $V(\varphi(\tau_i(z), z)) = (1 + 2i)/2$ and $\tilde{\rho}_i : S \to [0,1]$ by

$$\tilde{\rho}_i(z) = \begin{cases} 1 & \text{if } z \in R_i, \\ 0 & \text{if } z \in A_i, \\ \frac{1}{2} + \frac{1}{\pi}\tan^{-1}(\tau_i(z)) & \text{otherwise.} \end{cases}$$

In what follows we shall adopt the convention that $\tan \pm\frac{\pi}{2} = \pm\infty$. It is left to the reader to check that τ_i and $\tilde{\rho}_i$ are continuous.

Let $\mathcal{D} := \{(y_0, y_1) \in [0,1]^2 \mid 0 \leq y_i \leq 1,\ y_0 \geq y_1\}$. Define $\tilde{\rho} : S \to \mathcal{D}$ by

$$\tilde{\rho}(z) = (\tilde{\rho}_0(z), \tilde{\rho}_1(z)).$$

Obviously, $\tilde{\rho}$ is continuous, but it cannot be onto since $\tilde{\rho}_0(z) = \tilde{\rho}_1(z)$ if and only if $\tau_0(z) = \tau_1(z)$ which cannot happen. The following proposition, the proof of which follows straightforwardly from the definitions, summarizes the most important characteristics of $\tilde{\rho}$. See Figure 19.

Proposition 5.2

$$\begin{aligned}
\tilde{\rho}(z) = (1,1) &\quad\Leftrightarrow\quad z \in M(2)\\
\tilde{\rho}(z) = (1,0) &\quad\Leftrightarrow\quad z \in M(1)\\
\tilde{\rho}(z) = (0,0) &\quad\Leftrightarrow\quad z \in M(0)\\
\tilde{\rho}_0(z) = 1 &\quad\Leftrightarrow\quad z \in M(1,2)\\
\tilde{\rho}_1(z) = 1 &\quad\Leftrightarrow\quad z \in M(0,1)
\end{aligned}$$

We now define a flow $\tilde{\psi} : \mathbf{R} \times [0,1]^2 \to [0,1]^2$ by

$$\begin{aligned}
\tilde{\psi}(t, y_0, y_1) \;=\; & \left(\frac{1}{2}, \frac{1}{2}\right)\\
& + \frac{1}{\pi}\left(\tan^{-1}\left(-t + \tan(\pi(y_0 - \frac{1}{2}))\right), \tan^{-1}\left(-t + \tan(\pi(y_1 - \frac{1}{2}))\right)\right).
\end{aligned}$$

Observe that $\mathcal{D}$ is an invariant subspace of $[0,1]^2$ under $\tilde{\psi}$, and hence, to simplify the notation we shall also denote the restriction of $\tilde{\psi}$ to $\mathcal{D}$ by $\tilde{\psi}$.

Proposition 5.3 *The following diagram commutes.*

$$\begin{tikzcd}
\mathbf{R} \times S \arrow[r, "\varphi"] \arrow[d, "id \times \tilde{\rho}"'] & S \arrow[d, "\tilde{\rho}"] \\
\mathbf{R} \times \mathcal{D} \arrow[r, "\tilde{\psi}"] & \mathcal{D}
\end{tikzcd}$$

Proof: Consider the case $z \in M(2)$. We need to show that $\tilde{\rho}(\varphi(t,z)) = \tilde{\psi}(t, \tilde{\rho}(z))$. Since $M(2)$ is invariant $\varphi(t,z) \in M(2)$. Thus by Proposition 5.2, $\tilde{\rho}(\varphi(t,z)) =$

$(1,1)$. On the other hand

$$
\begin{aligned}
\tilde{\psi}(t,\tilde{\rho}(z)) &= \tilde{\psi}(t,1,1) \\
&= \left(\frac{1}{2},\frac{1}{2}\right) + \frac{1}{\pi}\left(\tan^{-1}(-t+\infty), \tan^{-1}(-t+\infty)\right) \\
&= (1,1).
\end{aligned}
$$

The cases where $z \in M(p)$ or $z \in M(p,p+1)$, $p = 0,1$ are handled similarly and the remaining situations are straightforward computations. ■

The following sets will prove useful later. Let

$$J_1^+ := [0,1]\times\{0\}\cup\{1\}\times[0,1]$$

and for $1/2 \le q < 1$, define

$$J_q^+ := \left(\bigcup_{q\le p<1}\tilde{\psi}(\mathbf{R},p,1-p)\right)\cup J_1^+ \subset \mathcal{D}.$$

Observe that for $q < 1$, $\tilde{\rho}^{-1}(J_q^+)$ is a neighborhood of the connecting orbits $M(2)\to M(1)$ and $M(1)\to M(0)$.

Similarly, let

$$J_1^- := [0,1]\times\{1\}\cup\{0\}\times[0,1]$$

and for $1/2 \le q < 1$ let

$$J_q^- := \left(\bigcup_{q\le p<1}\tilde{\psi}(\mathbf{R},1-p,p)\right)\cup J_1^-.$$

This finishes the general construction. In what follows we assume further information concerning either $M(1)$, $M(0,1)$, or $M(2,1)$.

5.1.1 $M(1) = M(1^+)\cup M(1^-)$

We now make the additional assumption that

$$\mathcal{M}(S) = \{M(p) \mid p = 0,1^\pm,2,\ 2 > 1^\pm > 0\}, \tag{10}$$

where $>$ represents the flow defined ordering. Observe that this forces the existence of $M(2)\to M(1^\pm)$ and $M(1^\pm)\to M(0)$ connections. Let

$$\Gamma^\pm := C(M(2),M(1^\pm))\cup C(M(1^\pm),M(0))\cup M(2)\cup M(1^\pm)\cup M(0).$$

By Proposition 5.2, $\tilde{\rho}(\Gamma^\pm) = J_1^+$.

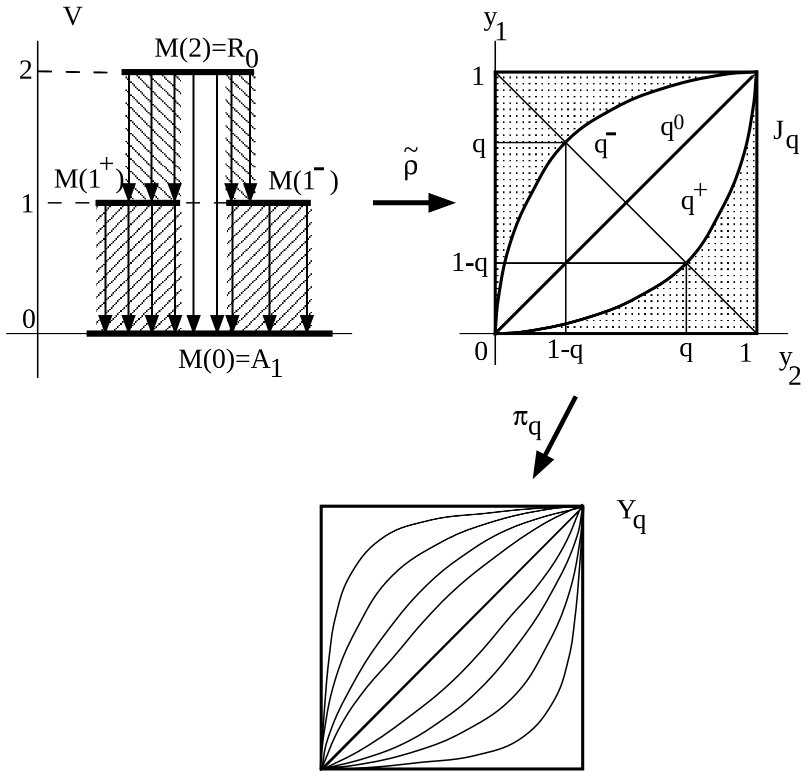

Figure 20: Map from the Morse decomposition onto J_q and Y_q.

The first step is to construct the image space and its flow for the semi-conjugacy. See Figure 20. Fix $1/2 \leq q < 1$. Let

$$J_q = J_q^+ \cup J_q^- \cup \{(y,y) \mid 0 \leq y \leq 1\} \subset [0,1]^2.$$

Observe that J_q is invariant under the flow $\tilde{\psi}$. As before we shall continue to denote the restriction of $\tilde{\psi}$ to J_q by $\tilde{\psi}$. There are three distinguished orbits on J_q,

- q^+ which passes through $(q, 1-q)$,
- q^- which passes through $(1-q, q)$, and
- q^0 which passes through $(1/2, 1/2)$.

These orbits will be identified pointwise as follows. Begin by setting

$$(q, 1-q) \in q^+ \quad \sim \quad (q,q) \in q^0 \quad \sim \quad (1-q, q) \in q^-.$$

Now given $y^+ \in q^+$, there exists a time $t(y^+)$ such that $\tilde{\psi}(t(y^+), y^+) = (q, 1-q)$. Then,

$$y^+ \in q^+ \quad \sim \quad \tilde{\psi}(-t(y^+), (q,q)) \in q^0.$$

Similarly, given $y^- \in q^-$, there exists a time $t(y^-)$ such that $\tilde{\psi}(t(y^-), y^-) = (1-q, q)$ and

$$y^- \in q^- \quad \sim \quad \tilde{\psi}(-t(y^-), (q,q)) \in q^0.$$

The induced quotient space,

$$Y_q := J_q / \sim,$$

is easily seen to be homeomorphic to $[0,1]^2$. Let $\pi_q : J_q \to Y_q$ be the associated quotient map and let

$$\psi : \mathbf{R} \times Y_q \to Y_q$$

be the flow induced by $\tilde{\psi}$ under the projection π_q.

Recall that the above construction was made under the assumption that $1/2 \leq q < 1$. Define

$$Y_1 := \partial[0,1]^2 \cup \{(y,y) \mid 0 \leq y \leq 1\}$$

and $\psi : \mathbf{R} \times Y_1 \to Y_1$ to be the restriction of $\tilde{\psi}$ to Y_1.

Let $U^\pm$ be neighborhoods of $\Gamma^\pm$ such that $\Gamma^\pm \not\subset U^\mp$. Assume that there exists $q < 1$ such that

$$\tilde{\rho}^{-1}(J_q^\pm) \subset U^\pm.$$

Let $W^\pm := \tilde\rho^{-1}(J_q) \cap U^\pm$ and define $r^\pm : W^\pm \to [0,1]^2$ by

$$\begin{aligned} r^+(z) &= (\tilde\rho_0(z), \tilde\rho_1(z)) \\ r^-(z) &= (\tilde\rho_1(z), \tilde\rho_0(z)). \end{aligned}$$

Finally, define $r^0 : S \setminus (W^+ \cup W^-) \to [0,1]^2$ by $r^0(z) = (\tilde\rho_0(z), \tilde\rho_0(z))$.

Define $\rho_q : S \to Y_q$ by

$$\rho_q(z) = \begin{cases} \pi_q \circ r^\pm(z) & \text{if } z \in W^\pm, \\ \pi_q \circ r^0(z) & \text{otherwise.} \end{cases}$$

Observe that ρ_q is continuous.

If there does not exist $q < 1$, then the above construction is performed with $q = 1$.

To simplify the notation, we shall refer to points in Y_q by their coordinates in $[0,1]^2$. It is easy to check that

$$\mathcal{M}(Y_q) := \{\Pi(2) = (1,1), \Pi(1^+) = (1,0), \Pi(1^-) = (0,1), \Pi(0) = (0,0) \mid 2 > 1^\pm > 0\}$$

is a Morse decomposition with the flow defined ordering of Y_q under ψ.

5.1.2 $M(1,0) = M^+(1,0) \cup M^-(1,0)$

In this part we return to the setting of only three Morse sets, however, we assume that we know that there are two isolated sets of connecting orbits from $M(1)$ to $M(0)$, the closure of which are denoted by $M^+(1,0)$ and $M^-(1,0)$. In analogy to the previous construction let

$$\Gamma^\pm := C(M(2), M(1^\pm)) \,\cup\, M^\pm(1,0) \,\cup\, M(2) \,\cup\, M(1^\pm) \,\cup\, M(0).$$

By Proposition 5.2, $\tilde\rho(\Gamma^\pm) = J_1^+$.

Let J_q be as in the previous subsection. To define the appropriate quotient space we use the same identification and *in addition* we set

$$(s,1) \sim (1,s).$$

The resulting quotient space,

$$Y_q^l := J_q / \sim,$$

is again homeomorphic to $[0,1]^2$. Let $\pi_q^l : J_q \to Y_q$ be the associated quotient map and let

$$\psi^l : \mathbf{R} \times Y_q^l \to Y_q^l$$

be the flow induced by $\tilde{\psi}$ under the projection π^l_q.

At the risk of being terribly redundant, let $U^\pm$ be neighborhoods of $\Gamma^\pm$ such that $\Gamma^\pm \not\subset U^\mp$. Assume that there exists $q < 1$ such that

$$\tilde{\rho}^{-1}(J_q^\pm) \subset U^\pm.$$

Let $W^\pm := \tilde{\rho}^{-1}(J_q) \cap U^\pm$ and define $r^\pm : W^\pm \to [0,1]^2$ by

$$\begin{aligned} r^+(z) &= (\tilde{\rho}_0(z), \tilde{\rho}_1(z)) \\ r^-(z) &= (\tilde{\rho}_1(z), \tilde{\rho}_0(z)). \end{aligned}$$

Finally, define $r^0 : S \setminus (W^+ \cup W^-) \to [0,1]^2$ by $r^0(z) = (\tilde{\rho}_0(z), \tilde{\rho}_0(z))$.

Define $\rho^l_q : S \to Y^l_q$ by

$$\rho^l_q(z) = \begin{cases} \pi^l_q \circ r^\pm(z) & \text{if } z \in W^\pm, \\ \pi^l_q \circ r^0(z) & \text{otherwise.} \end{cases}$$

If there does not exist $q < 1$, then the above construction is performed with $q = 1$.

It is easy to check that

$$\mathcal{M}(Y^l_q) := \{\Pi^l(2) = (1,1), \Pi^l(1) = (1,0) = (0,1), \Pi^l(0) = (0,0) \mid 2 > 1 > 0\}$$

is a Morse decomposition with the flow defined ordering of Y^l_q under ψ^l.

5.1.3 $M(2,1) = M^+(2,1) \cup M^-(2,1)$

This setting is similar to that of the previous subsection, however now it is assumed that there are two isolated sets of connecting orbits from $M(2)$ to $M(1)$ the closure of which are denoted by $M^+(2,1)$ and $M^-(2,1)$. Again, a quotient space Y^u_q is constructed from J_q, however the additional equivalence relation takes the form $(s,0) \sim (0,s)$. The corresponding quotient map is denoted by π^u_q and $\rho^u_q : S \to Y^u_q$ is defined by

$$\rho^u_q(z) = \begin{cases} \pi^u_q \circ r^\pm(z) & \text{if } z \in W^\pm, \\ \pi^u_q \circ r^0(z) & \text{otherwise.} \end{cases}$$

It is easy to check that

$$\mathcal{M}(Y^u_q) := \{\Pi^u(2) = (1,1), \Pi^u(1) = (1,0) = (0,1), \Pi^u(0) = (0,0) \mid 2 > 1 > 0\}$$

is a Morse decomposition with the flow defined ordering of Y^u_q under ψ^u.

5.2 Proof of Theorem 1.5

The proof will be given for $\mathcal{A}_{\mathcal{M}}(\mathrm{IV}_+)$ since the other case is analogous.

First observe that we are in the setting of subsection 5.1.2. There are two cases to consider. The first is that $q = 1$. Recall that we have a commutative diagram

$$\begin{array}{ccccccc}
\xrightarrow{\delta} & CH^p(M(2)) & \to & CH^p(S) & \to & CH^p(M(1,0)) & \to \\
 & \uparrow \rho_q^* & & \uparrow \rho_q^* & & \uparrow \rho_q^* & \\
\xrightarrow{\delta} & CH^p(\Pi(2)) & \to & CH^p(Y_1) & \to & CH^p(\Pi(0,1)) & \to
\end{array}$$

Since we have isomorphisms between $CH^p(M(1,0))$ and $CH^p(\Pi(0,1))$ and between $CH^p(M(2))$ and $CH^p(\Pi(2))$, the five lemma implies that $CH^p(Y_1^l)$ is isomorphic to $CH^p(S)$, a contradiction.

Thus it can be assumed that $q < 1$. For the rest of the argument fix $q \in (1/2, 1)$. We need to prove that $\rho_q : S \to Y_q^l$ is surjective. By assumption and the construction of the previous section it is clear that $\rho_q : M(1,0) \to \Pi(0,1)$ and $\rho_q : M(2) \to \Pi(2)$ surjectively. Thus, what needs to be studied are the connecting orbits from $M(2)$ to $M(1,0)$. To do this let $\Sigma = \{x \in S \mid V(x) = 3/2\}$. Observe that Σ is a local section for the flow and that every orbit in $C(M(2), M(1,0))$ intersects Σ.

Turning to the flow on Y_q^l, notice that there exists a unique $\lambda \in (1/2, 1)$ with the property that $(\lambda, 1/2) \in q^+$. Define $\Xi \subset Y_q^l$ by

$$\Xi := \{(y_1, 1/2) \mid \lambda \leq y_1 \leq 1\} \cup \{(1/2, y_2) \mid \lambda \leq y_2 \leq 1\}.$$

Observe that $\rho_q(\Sigma) \subset \Xi$ and that the proof is complete if it can be shown that ρ_q maps Σ onto Ξ.

Let

$$N := \{(y_1, y_2) \in Y_q^l \mid y_1 \geq \lambda \text{ and } y_2 \geq 1/2, \text{ or } y_2 \geq \lambda \text{ and } y_1 \geq 1/2\}.$$

Then, (N, Ξ) is an index pair for $\Pi(2)$.

Define $\hat{N} = \rho_q^{-1}(N)$, and $\hat{L} = \rho_q^{-1}(\Xi)$. Then, $(\hat{N}, \hat{L})$ is an index pair for $M(2)$. This gives rise to the following commutative diagram.

$$\begin{array}{ccccccccc}
\to & H^1(\hat{N}) & \to & H^1(\hat{L}) & \xrightarrow{\delta} & H^2(\hat{N}, \hat{L}) & \to & H^2(\hat{N}) & \to \\
 & \uparrow \rho_q^* & & \uparrow \rho_q^* & & \uparrow \rho_q^* & & \uparrow \rho_q^* & \\
\to & H^1(N) & \to & H^1(\Xi) & \xrightarrow{\delta} & H^2(N, L) & \to & H^2(N) & \to
\end{array}$$

Which can be rewritten as

$$\begin{array}{ccccccccc}
\to & 0 & \to & \mathbf{Z}_2 & \xrightarrow{\delta} & \mathbf{Z}_2 & \to & 0 & \to \\
 & \uparrow & & \uparrow \rho_q^* & & \uparrow \approx & & \uparrow & \\
\to & H^1(N) & \to & H^1(\Xi) & \xrightarrow{\delta} & H^2(N, L) & \to & H^2(N) & \to
\end{array}$$

This implies that ρ_q^* is injective. However, Ξ is homeomorphic to the circle S^1 and therefore $\rho_q : \Sigma \to \Xi$ is onto.

5.3 Proof of Theorem 1.8

The proofs of Theorem 1.8 (1) and (2) are identical due to the symmetry between $\mathcal{A}_{\mathcal{M}}(\mathrm{VII}_+)$ and $\mathcal{A}_{\mathcal{M}}(\mathrm{VII}_-)$, therefore we will only present the argument for the first setting. The proof naturally breaks into two cases depending upon the connection matrix.

5.3.1 The connection matrix is given by $\Delta(\mathrm{VII}_+)_1$

We shall show that there is a semi-conjugacy onto the planar dynamical system indicated in Figure 13(a).

From $\Delta(\mathrm{VII}_+)_1$ we conclude that the flow defined ordering is given by

$$C > C^a > A^{\pm}, \quad C > B^{\pm b} > C^b, \quad B^{-b} > A^-, \quad B^{+b} > A^+.$$

In particular $\{C, C^a, B^{-b}, A^-\}$, $\{C, B^{\pm b}, C^b\}$, and $\{C, B^{+b}, C^a, A^+\}$ are intervals.

Consider the isolated invariant set $M(C, C^a, B^{-b}, A^-)$. Under the identification $M(2) = C$, $M(1^+) = C^a$, $M(1^-) = B^{-b}$, and $M(0) = A^-$ this has a Morse decomposition as described in subsection 5.1.1. This leads to a map and quotient space

$$\rho_q^{A^-} : M(C, C^a, B^{-b}, A^-) \to Y_q^{A^-}$$

constructed exactly as in the earlier subsection. This can be done for $M(C, B^{\pm b}, C^b)$ and $M(C, B^{+b}, C^a, A^+)$, leading to maps $\rho_q^{C^b} : M(C, C^a, B^{-b}, A^-) \to Y_q^{C^b}$ and $\rho_q^{A^+} : M(C, C^a, B^{-b}, A^-) \to Y_q^{A^+}$, respectively. To define a semi-conjugacy on all of $\mathcal{A}_{\mathcal{M}}(\mathrm{VII}_+)$ we again form a quotient space by setting

$$\begin{aligned}
(1, y_2) \in Y_q^{A^-} &\sim (y_2, 1) \in Y_q^{A^+} \\
(1, y_2) \in Y_q^{A^+} &\sim (y_2, 1) \in Y_q^{C^b} \\
(1, y_2) \in Y_q^{C^b} &\sim (y_2, 1) \in Y_q^{A^-}.
\end{aligned}$$

Let

$$Y := \left(Y_q^{A^-} \cup Y_q^{A^+} \cup Y_q^{C^b}\right) / \sim$$

and let $\rho : S \to Y$ be the associated semi-conjugacy.

The proof that ρ is surjective now follows from the same arguments used in the proof of Theorem 1.5. In particular, one first considers the case where for one or more of the above Morse sets it is necessary to take $q = 1$. Looking at the long exact sequence for the attractor repeller pair with C as the repeller leads to a contradiction. Thus, it can be assumed that $q < 1$ for each of the Y_q^*. Again, let $\Sigma = \{x \in S \mid V(x) = 3/2\}$ (note that one may coarsen the Morse decomposition to one consisting of three Morse sets and thereby return to the general setting). One then constructs a local section Ξ by taking the union of the Ξ's constructed for each Y_q^* as 5.2. Once again, the union of the constructions on each Y_q^* gives rise to an index pair on Y which lifts to an index pair on $\mathcal{A}_{\mathcal{M}}(\mathrm{VII}_-)$. The corresponding long exact sequence is used to show that ρ maps Σ surjectively onto Ξ.

5.3.2 The connection matrix is given by $\Delta(\mathrm{VII}_+)_2$

The difficulty in this case is that the connection matrix information is not sufficient to determine the flow defined ordering. Thus, we begin by assuming that there are no connecting orbits from C to $M(B^{\pm b}, A^{\pm})$ and will prove that Figure 13(b) indicates the appropriate semi-conjugacy. By symmetry and the fact that the connection matrix entries corresponding to C^a are zero, this implies that there is a double connection from C^a to C^b and no connections from C^a to $M(B^{\pm b}, A^{\pm})$. Hence the flow defined order is given by

$$C > C^a > C^b, \quad B^{+b} > A, C^b, \quad B^{-b} > A^-, C^b.$$

This in turn implies that we have intervals $\{C, C^a, C^b\}$, $\{B^{+b}, A, C^b\}$, and $\{B^{-b}, A^-, C^b\}$. The dynamics on the isolated invariant sets $M(B^{+b}, A, C^b)$ and $M(B^{-b}, A^-, C^b)$ are as indicated in Figure 13(b) since $B^{\pm}$ have one dimensional unstable manifolds. The semi-conjugacy for $M(C, C^a, C^b)$ follows from an argument identical to that of 5.2.

We now consider the case where there are connecting orbits from C to $M(B^{\pm b}, A^{\pm})$. The flow defined order now becomes

$$C > B^{\pm b} > C^b, \quad C > C^a > C^b, \quad B^{+b} > A^+, \quad B^{-b} > A^-.$$

Observe that $\{C, B^{\pm b}, A^{\pm}\}$ is an interval under this ordering. Thus, we can form the isolated invariant set $M(*) := M(C, B^{\pm b}, A^{\pm})$ and obtain a coarser Morse decomposition of $\mathcal{A}$ consisting of the Morse sets $\{M(*), C^a, C^b\}$ with the ordering $M(*) > C^a > C^b$. Since we still have the pair of connecting orbits from C^a to C^b we are in the setting of section 5.1.2 which gives the semi-conjugacy indicated in Figure 13(c).

Observe that in this case all of $M(*)$ is mapped onto a single equilibrium point under the semi-conjugacy. Obviously, considerable information is lost in this process. Numerically, however, we observe that the global attractor of the shadow system restricted to the monotone solution subspace is a two dimensional graph. Under this assumption we can think of $\mathcal{A}_{\mathcal{M}}(\mathrm{VII}_+)$ as being embedded in the plane. Furthermore, we assume that there are connecting orbits from C to $M(B^{\pm b}, A^{\pm})$. Since C has a two dimensional unstable manifold and $B^{\pm}$ have one dimensional unstable manifolds a $C \to B^{\pm}$ connection is necessarily transverse. However, the connection matrix entry corresponding to C to $B^{\pm}$ connection is zero, therefore, there must an even number of connecting orbits. Again the fact that $\mathcal{A}_{\mathcal{M}}(\mathrm{VII}_+)$ can be thought of as lying in the plane implies that there are exactly two connecting orbits. Therefore the flow defined order becomes $C > B^{\pm b} > C^b$, $B^{+b} > A^+$, $B^{-b} > A^-$, $C > C^a > C^b$. Observe that we have the following intervals $\{C, C^a, B^{-b}, C^b\}$, $\{C, C^a, B^{+b}, C^b\}$, $\{C, B^{-b}, A^-\}$, $\{C, B^{+b}, A^+\}$, and $\{C, B^{-b}, B^{+b}, C^b\}$, and hence the following isolated invariant sets $M(C, C^a, B^{-b}, C^b)$, $M(C, C^a, B^{+b}, C^b)$, $M(C, B^{-b}, A^-)$, $M(C, B^{+b}, A^+)$, and $M(C, B^{-b}, B^{+b}, C^b)$. To each such isolated invariant set we will associate a semi-conjugacy constructed as described in 5.1.

$$
\begin{aligned}
\rho_q[-] &: M(C, C^a, B^{-b}, C^b) \to Y_q[-] \\
\rho_q[+] &: M(C, C^a, B^{+b}, C^b) \to Y_q[+] \\
\rho_q &: M(C, B^{-b}, B^{+b}, C^b) \to Y_q \\
\rho_q^u[+] &: M(C, B^{+b}, A^+) \to Y_q^l[+] \\
\rho_q^u[-] &: M(C, B^{-b}, A^+) \to Y_q^l[-]
\end{aligned}
$$

The proof now follows from the same types of arguments as in the previous subsection.

5.4 Proof of Theorem 1.9

The proof of this Theorem mimics the proof of Theorem 1.8.

6 Discussions

In this paper we have succeeded in classifying, up to semi-conjugacies, the dynamics in the shadow system restricted to the positively invariant subspace consisting of monotone solutions. This classification was obtained by using the ideas from the Conley index theory and is based on a decomposition of the parameter space in terms of local bifurcations of stationary solutions for the specific nonlinearity given in §1. However, the same kind of results should also hold for more general cases with different nonlinearities. The result of the classification shows that we have a unique global connecting orbit structure in each of the regions given by the local stationary bifurcations, except, perhaps, in the regions $VII_{\pm}$ and $VIII_{\pm}$ where we have three possibilities of the semi-conjugacy models, respectively. More precisely, we have shown that there exist two types of connecting orbit structures in the region $VIII_0$ where the system admits the extra odd symmetry, and the results of the numerical computation of a robust connecting orbit determine one of them. This yields the unique semi-conjugacy model for region $VIII_0$. When one enters into the regions $VIII_{\pm}$ from $VIII_0$ another connection matrix becomes possible which, in turn, gives rise to the possibility of additional semi-conjugacy models for the global attractors. Similar multiple semi-conjugacy models are, also, possible in the regions $VII_{\pm}$. This is interesting, because it indicates that there is a chance that a global bifurcation, in the form of a saddle-saddle connection, can take place. More precisely, the semi-conjugacy model in the region $VIII_0$ ($\mu = 0$) will remain valid for small but non-zero μ in $VIII_{\pm}$. If, however, for larger μ a different semi-conjugacy model is required, then a saddle-saddle connection between $B^{\pm a}$ and $B^{\pm b}$ must occur.

Which of these three models really occurs in the regions $VII_{\pm}$ and $VIII_{\pm}$ is determined by the saddle-node bifurcation involving $A^{\pm}$ and $B^{\pm a}$ (or $A^{\pm}$ and $B^{\pm b}$ in regions VII_{-} and $VIII_{-}$) and where it occurs with respect to a connecting orbit that persists throughout the bifurcation. To be more specific, consider the transition from region V_{+} to $VIII_{+}$. At the joint boundary of these two regions a saddle-node bifurcation, through which the stationary solutions $A^{\pm}$ and $B^{\pm a}$ are born in pairs, occurs. It seems quite natural to believe that the location of this saddle-node bifurcation is independent of the location of the connections $B^{\pm b} \to C^b$ which persist in the course of the bifurcation. Therefore, generically we expect that $A^{\pm}$ and $B^{\pm a}$ do not lie on these connecting orbits. This is the case corresponding to the semi-conjugacy models depicted in Figure 16(b) and (c) or (d). On the other hand, the remaining possibility, Figure 16(a), corresponds to the case where the saddle-node bifurcation occurs precisely on the connecting orbit. One expects this to be a highly non-generic situation. With this in mind we examined more carefully the relation between the saddle-node bifurcation and the connecting orbit.

The connecting orbits can be visualized by taking the projection $\pi : (u, \xi) \mapsto (\bar{u}, \xi)$ and Figure 21 shows the projected picture of the connecting orbits in region $VIII_{+}$. Since π is invariant with respect to the Neumann symmetry, the two connecting orbits $A^{\pm} \to B^{\pm a}$ are projected to a single curve as in Figure 21. Surprisingly, these stationary solutions seem to appear precisely on the connecting orbits $B^{\pm b} \to C^b$, indicating that the saddle-node bifurcation appears in a non-generic manner.

In order to see this situation more explicitly, we computed two unstable eigenfunctions for the stationary solution C and projected the whole connecting

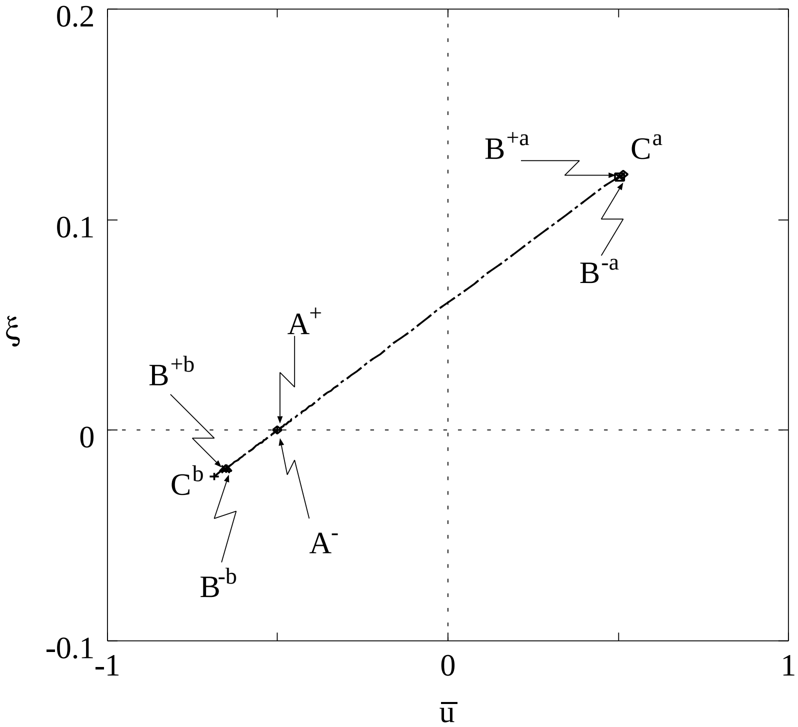

Figure 21: Projection of connections to $(\bar{u}, \xi)$-space with $k = 0.5,\ \varepsilon = 0.01,\ \lambda = 0.12,\ \mu = 0.06$

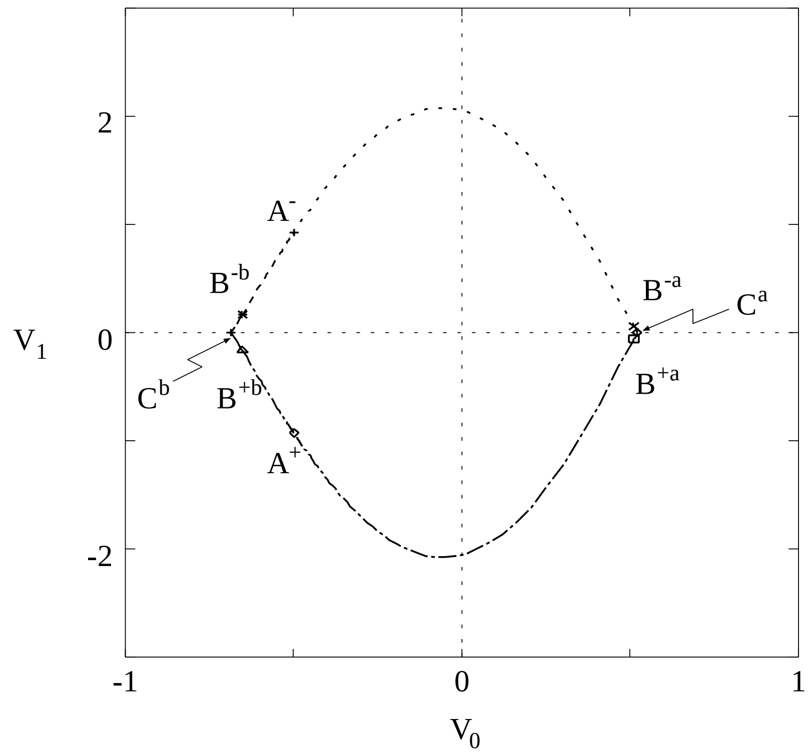

Figure 22: Projection of connections to (v_0, v_1)-space with $k = 0.5$, $\varepsilon = 0.01$, $\lambda = 0.12$, $\mu = 0.06$

orbits onto the subspace spanned by these eigenfunctions. To be more precise, recall that ρ_0 and ρ_1 are the unstable eigenvalues corresponding to the monotone eigenfunctions at the stationary solution C. Consider the subspace spanned by the corresponding eigenfunctions v_0 and v_1. Figure 22 exhibits the connecting orbit structure projected to the (v_0, v_1)-subspace with parameter values in the region VIII_+, whereas Figure 23 does that in the region V_+. One observes that the stationary solutions $A^{\pm}$ and $B^{\pm a}$ are located on the $B^{\pm b} \to C^b$ connecting orbits. These numerical results strongly suggest that the transition from $\mathrm{V}_{\pm}$ to $\mathrm{VIII}_{\pm}$ occurs in the above mentioned degenerate manner. If this is the case, then the two generic semi-conjugacy models cannot occur, and therefore, we once again have a unique connecting orbit structure over the entire region $\mathrm{VIII}_{\pm}$.

The degeneracy of the transition remains persistent under variation of parameter values and even under variation in the nonlinearities of the shadow system. This forces us to consider that such a degeneracy occurs because the

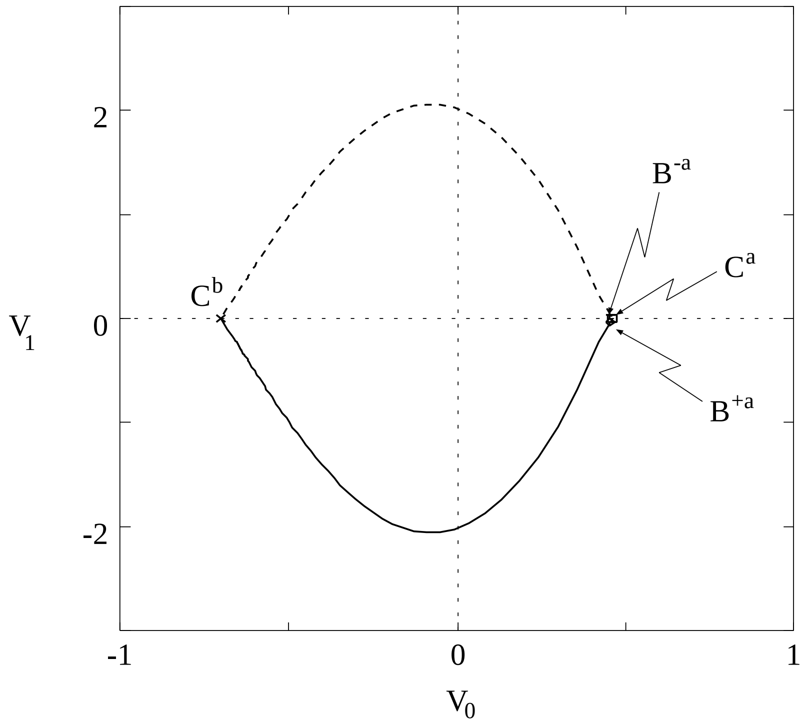

Figure 23: Projection of connections to (v_0, v_1)-space with $k = 0.5,\ \varepsilon = 0.01,\ \lambda = 0.12,\ \mu = 0.08$

shadow system possesses an unknown restriction such as a hidden symmetry, or more likely some type of monotonicity which is similar to that in the scalar reaction diffusion equation. So far we have been unable to determine this mysterious constraint, although we have tested various possibilities. We conclude this paper by giving conjectures and open problems and leave them for future study.

Conjecture 1: The shadow system studied in this paper is a Morse-Smale system except at the local bifurcations of stationary solutions. Namely, no global bifurcations involving saddle-saddle connections occur.

Conjecture 2: The global attractor of the shadow system restricted to the monotone solution subspace is a two-dimensional graph.

Problem 1: Conduct a similar study for solutions with at most k monotone intervals. Note that such solutions form a positively invariant subspace as in the case of the monotone solutions.

Problem 2: The shadow system is a singular limit of a system of reaction-diffusion equations with one of the diffusion coefficients going to infinity. Since one expects upper semi-continuity of global attractors, it is reasonable to expect that the semi-conjugacy models persist as well. Thus the problem is to extend the results of the shadow system to the system of reaction diffusion equations with very large but finite diffusivity for the inhibitor. Some studies in this direction have already been done. For instance, Hale and Sakamoto [9] have proven that the global attractors persist under this type of singular perturbation. The Morse decomposition of the global attractor should also be persistent. Can one show that our semi-conjugacy models persist as well?

References

[1] L. Arnold, C. Jones, K. Mischaikow, and G. Raugel, *Dynamical Systems; Montecatini Terme 1994*, R. Johnson, ed., Lect. Notes Math. 1609, Springer, 1995.

[2] P. Brunovský and B. Fiedler, Connecting orbits in scalar reaction diffusion equations, *Dynamics Reported*, Vol. 1 (1988), 57–90, Wiley.

[3] C. Conley, *Isolated Invariant Sets and the Morse Index*, CBMS Lecture Notes, Vol. 38, 1978, A. M. S.

[4] R. Franzosa, Index filtrations and the homology index braid for partially ordered Morse decompositions, Trans. A. M. S. **298** (1986), 193–213.

[5] R. Franzosa, The connection matrix theory for Morse decompositions, Trans. A. M. S. **311** (1989), 561–592.

[6] R. Franzosa, The continuation theory for Morse decompositions and connection matrices, Trans. A. M. S. **310** (1988), 781-803.

[7] R. Franzosa and K. Mischaikow, Algebraic transition matrices, Trans. A. M. S. (to appear).

[8] R. Gardner, Y. Nishiura, and T. Tsujikawa, unpublished.

[9] J. K. Hale and K. Sakamoto, Shadow systems and attractors in reaction-diffusion equations, Appl. Anal. **32** (1989), 287–303.

[10] H. Hattori and K. Mischaikow, A dynamical system approach to a phase transition problem, J. Dynam. Diff. Eq. **94** (1991), 340–378.

[11] H. Matano, Asymptotic behavior and stability of solutions of semilinear diffusion equations, Publ. RIMS Kyoto Univ. **15** (1979), 401-454.

[12] C. McCord, Mappings and homological properties in the homology Conley index, Ergod. Th. Dynam. Sys. **8*** (1988), 175–198.

[13] C. McCord, Mappings and Morse decompositions in the homology Conley index, Indiana Univ. Math. J. **40** (1991), 1061–1082.

[14] C. McCord, The connection map for attractor repeller pairs, Trans. A. M. S. **307** (1988), 195–203.

[15] C. McCord and K. Mischaikow, Connected simple systems, transition matrices, and heteroclinic bifurcations, Trans. A. M. S. **333** (1992), 379–422.

[16] C. McCord and K. Mischaikow, On the global dynamics of attractors for scalar delay equations, Jour. A. M. S. (to appear).

[17] K. Mischaikow, Global asymptotic dynamics of gradient-like bistable equations, SIAM J. Math. Anal. **26** (1995), 1199–1224.

[18] Y. Nishiura, Global structure of bifurcating solutions of some reaction-diffusion systems, SIAM J. Math. Anal. **13** (1982), 555–593.

[19] Y. Nishiura, Coexistence of infinitely many stable solutions to reaction diffusion systems in the singular limit, in *Dynamics Reported* Vol. 3 (New Series), 1994, pp. 25–103, Springer.

[20] Y. Nishiura, Global structure of bifurcating solutions of some reaction-diffusion systems and their stability problem, *Computing Methods in Applied Sciences and Engineering, V*, Eds. R. Glowinski and J. L. Lions, pp. 185 – 204, 1982, North-Holland.

[21] Y. Nishiura and T. Tsujikawa, Instability of singularly perturbed Neumann layer solutions in reaction-diffusion systems, Hiroshima Math. J. **20** (1990), 297-329.

[22] K. P. Rybakowski, *The Homotopy Index and Partial Differential Equations*, 1987, Universitext, Springer-Verlag.

[23] D. Salamon, Connected simple systems and the Conley index of isolated invariant sets, Trans. A. M. S. **291** (1985), 1–41.

[24] J. Smoller, *Shock Waves and Reaction Diffusion Equations*, 1980, 2nd Edition 1994, Springer-Verlag.

[25] J. Smoller and A. Wasserman, Global bifurcation of steady-state solutions, J. Diff. Eq. **39** (1981), 269–290.